Current frameworks for reference ET and crop coefficient calculation

R G. Allen
University of Idaho, RAllen@kimberly.uidaho.edu

Ayse Kilic
University of Nebraska-Lincoln, akilic@unl.edu

Clarence W. Robison
University of Idaho

2950 Niles Road, St. Joseph, MI 49085-9659, USA
269.429.0300 fax 269.429.3852 hq@asabe.org www.asabe.org

An ASABE Meeting Presentation
DOI: https://doi.org/10.13031/irrig.2020-070
Paper Number: 20-070

Current frameworks for reference ET and crop coefficient calculation

Richard G. Allen[1] Ayse Kilic[2], and Clarence W. Robison[3]

[1] Professor of Water Resources Engineering, University of Idaho, Kimberly, Idaho USA 83341. RAllen@kimberly.uidaho.edu
[2] Professor of Civil Engineering and School of Natural Resources, Lincoln, NE 68516
[2] Research Associate, University of Idaho, Kimberly, Idaho USA 83341.

Written for presentation at the
6th Decennial National Irrigation Symposium
Sponsored by ASABE
San Antonio, Texas
November 30 – December 4, 2020

ABSTRACT. This article describes current and likely near-term future frameworks for calculating evapotranspiration. These include structures for estimating crop coefficients (K_c) primarily centered on the FAO-56 dual K_c approach, with example applications. Emphasis is placed on estimation of parameters and special cases to be considered. Newer, and often preferred, bases for establishing K_{cb} curves include thermal units and vegetation indices. Also described and discussed are the application of reference ET calculations using hourly vs. 24-hour timesteps, the use of and conditioning of gridded weather data sets, and the likelihood of movement toward multi-layer and multi-source resistance models for ET estimation. Complementing this is satellite-based determination of ET using both vegetation indices and surface energy balance.

Keywords. ***consumptive use, dual crop coefficient, evapotranspiration, FAO-56, irrigation water requirements, remote sensing, gridded weather data***

[1] Professor of Water Resources Engineering, University of Idaho, Kimberly, Idaho USA 83341. RAllen@kimberly.uidaho.edu

INTRODUCTION

Estimation of evapotranspiration is under continual development and evolution, with significant developments and standardizations made during the past three decades for both reference ET (ET_{ref}) and for crop coefficients (K_c). These standardizations provide consistency and reproducibility in estimating ET_{ref} and a consistent basis for determining and expressing K_c curves, especially at the local scale. The application of the dual K_c procedure is growing, and has strong potential for improving accuracy of ET estimates as compared to the single K_c approach.

This article describes current structures for estimating crop coefficients including the standardized FAO-56 dual K_c approach, with example applications. Emphasis is placed on estimation of parameters and special cases to be considered. Newer bases for establishing K_{cb} curves include thermal units and vegetation indices.

Background

The crop coefficient (K_c) times reference ET (ET_{ref}) method is a consistent, robust calculation procedure for estimating evapotranspiration (ET), where the ET_{ref} component represents the ET from a hypothetical reference surface (Allen et al., 1998; ASCE, 2005, 2016). ET_{ref} is generally calculated using a physically based equation such as the Penman-Monteith (ASCE 1990; 2005; 2016). The crop coefficient component encapsulates the major differences between the ET behavior of the crop and ET behavior of the reference crop, including differences caused by incomplete ground cover, different leaf area, different bulk stomatal conductance or aerodynamic roughness and wetness of exposed soil. The K_c ET_{ref} procedure strikes a pragmatic compromise between using a completely physical basis where a number of crop specific parameters must be presented that may vary with crop variety and location and that do change over time, and a simple, bulked crop coefficient relationship. The calculation of ET_{ref} is straightforward and standardized and incorporates the primary impacts of weather on the ET rate (ASCE 2005; 2016). The K_c, in turn, can be expressed as a relatively simple, continuous function over the growing season and is readily visualized by all levels of users.

The K_c ET_{ref} relation was proposed in the 1960's, clarified by Jensen (1968), and first used in a computerized irrigation scheduling program by Jensen (1969; Jensen et al. 1970, 1971). Those first applications utilized a single K_c approach. Prior to that, K_c curves, such as those associated with the SCS TR-21 Blaney-Criddle method, largely had a nonreference crop basis (Hargreaves, 1948; Veihmeyer and Hendrickson, 1955; Erie et al., 1965, 1982, USDA, 1967). The more dependable reference-based K_c curves were often developed based on daily ET measured with lysimeters that were then related to a grass or alfalfa reference ET. Some K_c curves were refined for conditions of a dry surface soil, or when the soil visually appeared to be dry, and were called *basal crop* coefficients (Wright, 1982). More accurate ET estimates could be obtained using basal coefficients with subsequent adjustment for the wetness of the surface soil for several days following rains or irrigation. This process is referred to as the dual K_c approach (Wright, 1982; Allen et al., 1998).

The primary factor causing an increase in the crop coefficient is an increase in plant cover or leaf area per unit ground area (LAI) as the crop develops. Increased leaf area results in a decrease in bulk surface resistance and an increase in captured solar radiation and aerodynamic exchange. Most publications on crop coefficient curves have presented K_c as a function of some form of an absolute or scaled time basis. Other studies have related the rate of increases in LAI and therefore K_c for various crops as a function of accumulated daily weather such as cumulative degree days.

An upper limit on K_c

One of the benefits of the K_c ET_{ref} approach is that ET_{ref} represents a near maximum on expected ET based on atmospheric demands and the definition of the reference surface. Therefore, one should expect to find an upper physical limit on K_c. When applying the standardized Penman-Monteith (PM) reference ET equation under humid conditions, where a majority of energy for the ET process is from net radiation, the K_c for large expanses of similar vegetation does not exceed about 1.0 to 1.1 when used with the alfalfa reference and about 1.2 when used with the grass reference. In dry climates, where additional advection of warm dry air can occur to increase ET from irrigated surfaces, the K_c still does not exceed about 1.0 to 1.1 for the alfalfa reference but can reach maximum values of about 1.3 to 1.4 when used with the aerodynamically smoother grass reference. The reason for the near-constant 1.0 to 1.1 crop coefficients for the alfalfa reference is that the alfalfa reference crop has about the same albedo, LAI, and roughness as most agricultural crops at full cover and therefore converts similar amounts of radiant energy and sensible heat to vapor transfer, including impacts of advection. An expanse of reference crop (especially alfalfa) will approach the maximum conversion of available energy into total latent energy, λE, representing ET, so that the ratio of λE for any other tall, leafy, well-watered crop to alfalfa λE will be near 1.0. This observation is born out in viewing the maximum values for K_{cb} reported by Wright (1982) shown in Figure 1, where none of Wright's K_{cb}s, based on the alfalfa reference, exceeded 1.03 when averaged over weekly or longer periods. In the case of the grass reference, where the vegetation is shorter and LAI may be less, values for K_{cb} may approach 1.3 for tall, dense crops under arid and semiarid conditions (Doorenbos and Pruitt, 1977; Allen et al., 1998). Values reported for K_c that exceed about 1.1 for use with ET_r and about 1.3 to 1.4 for use with ET_o should give cause for questioning the reported K_c values in terms of accuracy or bias in the experimental or environmental basis (Allen et al., 2011a; 2001b; ASCE, 2016).

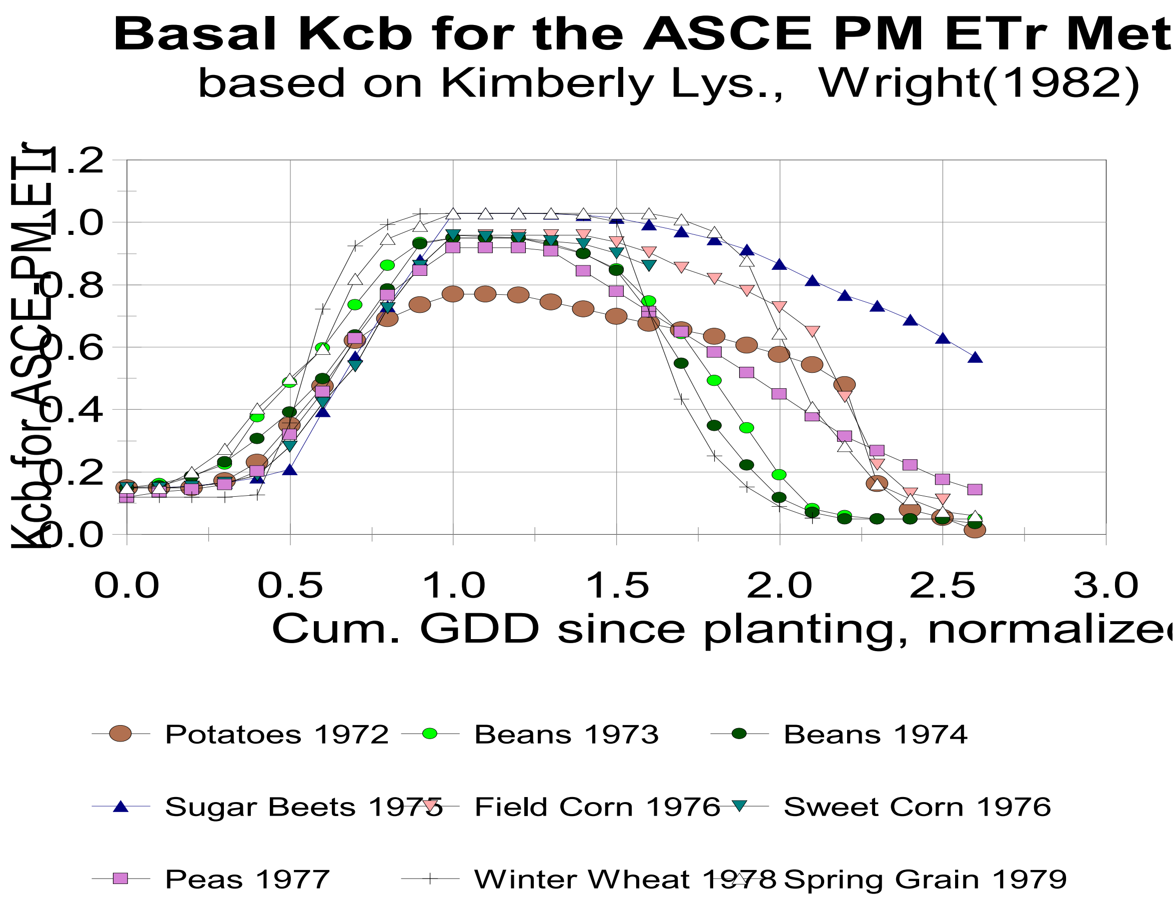

Figure 1. Basal crop coefficients, K_{cb}, developed by Wright (1982) for irrigated crops common to southern Idaho. The values are plotted relative to the fraction of cumulative growing degree days (GDD) since planting that is normalized to time of attaining full cover so that the normalized cumulative GDD (NCGDD) is 1.0 at attainment of effective full cover (Allen and Wright, 2006)

General crop coefficient curves

Generalized crop coefficient curves for estimating crop ET_c for crops or other vegetation are shown in Fig.2. The K_{cb} curve represents a "basal" crop coefficient for conditions where the soil surface is visually dry, so that evaporation from soil is minimal, but where the availability of soil water does not limit plant growth or transpiration. This curve represents a minimum ET_c situation for adequate soil water. The "spikes" in Fig. 2 represent occurrences of precipitation or irrigation that wet the soil surface and temporarily increase total ET_c for one to five days. The spikes decay to the K_{cb} curve as the soil surface dries. The spikes generally approach a maximum value of 0.8 to 1.0 for an alfalfa ET_r basis (Wright, 1982) and 1.0 to 1.2 for a grass ET_o basis (Allen et al. 1998). The K_{cm} curve in Fig. 2 represents a so-called "mean" crop coefficient that includes averaged effects of the wet soil spikes under specific rainfall and irrigation frequencies. Sometimes the K_{cm} is referred to as the "single" K_c. The final, "limited soil water" curve in the figure represents the decrease in ET_c when plant water uptake and ET is limited by available soil water.

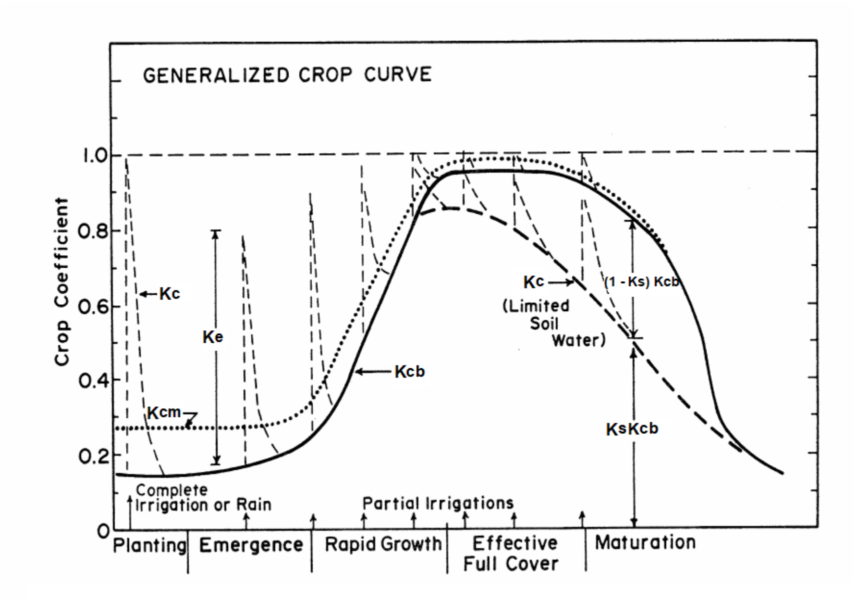

Figure 2. Generalized cover coefficient curves showing the effects of growth stage, wet surface soil and limited available soil water. Source: Wright (1982); Jensen et al. (1990).

PROCEDURE

The use of K_{cb} curves requires adjustment for wet soil effects after rain or irrigation. This results in more accurate estimates of ET_c on a daily basis for use in soil water modeling and irrigation scheduling than using mean coefficients in which the effects of local rainfall or irrigation frequencies are included. The total crop coefficient, K_c is computed from K_{cb} in the dual K_c procedure (Allen et al., 1998) as

$$K_c = K_s K_{cb} + K_e \tag{1}$$

where K_s is a dimensionless coefficient dependent on available soil water, and K_e is a coefficient to adjust for increased evaporation from wet soil immediately after rain or irrigation. The value for K_s is 1.0 unless available soil water limits transpiration, in which case it has a value less than 1.0. A potential ET_c is estimated as $ET_c = K_c\ ET_{ref}$ when K_s in Eq. (1) is set to 1.0. Actual ET, ET_a, is estimated as $ET_a = K_c\ ET_{ref}$ where K_s in Eq. (1) might be less than 1.0. The values for K_e represent the "spikes" shown in Fig. 2. Estimation of K_e for bare soil conditions is described in detail in Allen et al. (1998), Allen (2011) and Jensen and Allen (2016). Most current practices estimate K_e by conducting an hourly or daily water balance of a surface soil slab and proportioning K_e according to moisture remaining in the slab during stage 2 drying (Allen et al., 1998; Allen 2011).

In basin-wide water balance studies or irrigation system planning, use of mean, or single, crop coefficients may be more useful and convenient than computing a daily K_c based on a combination of K_{cb}, K_s and K_e as used in the dual K_c method of Eq. (1). The mean crop curve, K_{cm}, shown in Fig. 2, lies above the basal curve by an amount that depends on the frequency of soil wetting. When a mean coefficient is used, usually no additional adjustment is possible for the effects of surface soil wetness. Adjustments can be made for the effects of limited soil water as

$$K_c = K_s K_{cm} \tag{2}$$

Values for K_{cm} during partial crop cover are dependent on precipitation frequency and irrigation practices that wet all or part of the soil surface. Therefore, published values for K_{cm} do not have high accuracy when transferred among climates or irrigation practices. More accurate and representative K_{cm} curves can be generated using K_{cb} curves and the dual K_c procedure for known or simulated precipitation or irrigation frequencies. They can also be determined by sampling ET_c from populations of fields using satellite-based remote sensing (Tasumi et al., 2005; Tasumi and Allen, 2007; Singh and Kilic-Irmak, 2009).

Linear FAO K_c *model*

Although several crop coefficient models have used a curvilinear curve shape, the linear segment model proposed by the FAO is widely used and is easy to formulate. A side-by-side comparison of daily K_c calculated using the dual K_c method with a curvilinear K_{cb} curve and the linear segment model is shown in Fig. 3 for a sweet corn crop in southern Idaho. Daily measurements by precision weighing lysimeter by J.L.Wright, USDA-ARS (ret.) are shown. Agreement with measurements is relatively good for both curvilinear and piece-wise linear K_{cb} models, including increases during periods following wetting events. K_s in the Kimberly application was assumed to be 1.0, although the sweet corn crop may have experienced some stress around day of year 230. The crop also experienced hail damage near that date.

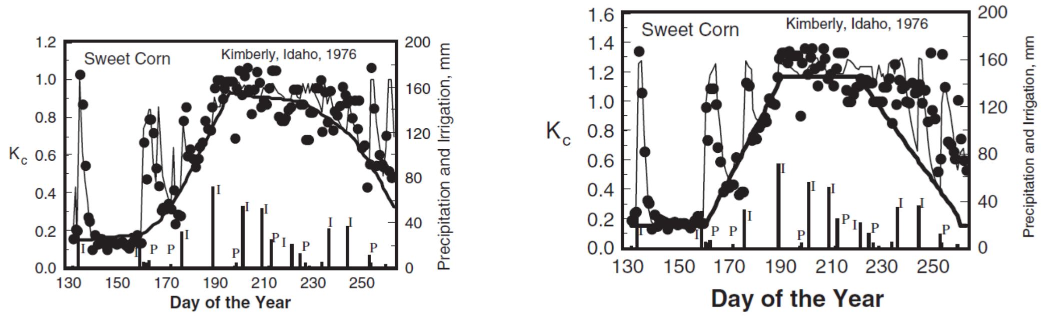

Figure 3. Daily K_c estimated with the dual K_c method for a sweet corn crop near Kimberly, Idaho during 1976 using a curvilinear K_{cb} curve with alfalfa reference ET_r basis (left) and using a linear segment K_{cb} curve with clipped grass reference ET_o basis (right). Black symbols represent daily measurement by precision weighing lysimeter by J.L.Wright, USDA-ARS (ret.) (personal communication). The thick line is K_{cb} and the thin line is $K_{cb} + K_e$. K_s was assumed to be 1.0.

The procedure for constructing the linear-segment K_c curve was presented in FAO 24 (Doorenbos and Pruitt 1977) and FAO 56 (Allen et al. 1998). In the FAO procedure, a K_c or K_{cb} curve such as that shown in Fig. 3 is constructed. Only three tabularized values for K_c are required to describe and construct the curve. $K_{c\ mid}$ or $K_{cb\ mid}$ represents the average value for K_c or K_{cb} expected during the total midseason period, rather than an absolute peak daily value reached by the crop. The four crop growth stages are generally characterized in terms of benchmark crop growth stages or cultivation practices. Values for K_c or K_{cb} during the initial, midseason and end of growing season periods, denoted as $K_{c\ ini}$, $K_{c\ mid}$, and $K_{c\ end}$ and $K_{cb\ ini}$, $K_{cb\ mid}$, and $K_{cb\ end}$ are provided in Allen et al. (1998) and in Appendix B and D of ASCE (2016).

The straight-line K_{cb} curve method of FAO method is generally appropriate for most applications. Hunsaker (1999) developed and compared K_{cb} curves for a cotton crop in Arizona using the straight-line method of FAO and curvilinear curves based on days after planting and based on cumulative growing degree days. He concluded that any of the three K_{cb} curve construction methods can result in good estimates of daily ET_c for the early-maturity cotton measured, when grown under climatic conditions similar to those of the study and when using appropriate starting dates.

Estimating time-bases for K_c models

FAO 24 (Doorenbos and Pruitt 197) and FAO 56 (Allen et al. 1998) provided general lengths for growth (development) stages for various types of climates and locations. Appendix C of ASCE (2016) summarized this information. The rate of vegetative development and attainment of effective full cover is affected by weather conditions, especially by mean daily air temperature (Ritchie and NeSmith 1991). Therefore, the length in time between planting or plant emergence and effective full cover for various crops or other vegetation will vary with climate, latitude, elevation, and planting date (if cultivated) and with species and cultivar (variety). Generally, once effective full cover for a plant canopy has been reached, the rate of phenological development (flowering, seed development, ripening, and senescence or death of leaf tissue) often proceeds at a rate that depends on plant genotype rather than weather (Wright 1982).

In many situations, the emergence of vegetation, greenup, and attainment of effective full cover can be estimated using cumulative degree-based regression equations or plant growth models (Sinclair, 1984; Sammis, 1985; Snyder, 1985; Flesch and Dale, 1987; Ritchie and NeSmith, 1991; Ritchie, 1991; Slack et al., 1996; Snyder et al., 1999; Cesaraccio et al., 2001; Spano et al., 2002; Sammis et al., 2004; Allen and Robison, 2007; Allen et al., 2020a). The use of cumulative growing degree days provides an automated and quantitative stretching or shrinkage of the generated K_c curves for years or growing seasons that run cooler or warmer than average. That year-to-year variation in the time base increases accuracy of ET estimation.

Wright (2001) and Allen and Wright (2006) converted the Wright (1982) K_{cb} curves shown in Figure 1 into cumulative growing-degree-day (CGDD)-based curves where the K_{cb} values for the growing season were expressed as a ratio of the CGDD required for the crop to develop from the date of planting or greenup until effective full cover. The winter wheat curve of Allen and Wright (2006) was applied by Allen and Robison (2007) during the Idaho winter by beginning the curve in October, with reductions in CGDD applied when T_{min} fell below threshold values during cold winter periods (Allen et al., 2020a). The reductions in CGDD during cold periods effectively reset CGDD and estimated phenological development by a few days to a few weeks.

Appendix F of ASCE (2016) provides K_c curves traceable to Wright (1981, 1982) for Kimberly, Idaho, that were converted to a normalized cumulative growing degree day basis. Normalization of CGDD was pioneered by Wright (2001) and is accomplished by dividing CGDD on any day by the CGDD required to reach effective full cover. That results in a

NCGDD equal to 1.0 at attainment of effective full cover and produces scaled K_{cb} such as shown in Figure 1. Those scaled K_{cb} curves are apt to be more transferable to other climates and years than straight time-based curves due to their thermal basis. Values for CGDD at effective full cover were reported by Wright (2001) and Allen and Wright (2006), Allen and Robison (2007), ASCE (2016) and Allen et al., (2020a). Those values for CGDD can be adjusted for different crop varieties or for different regions of the US, similar to what was done by Huntington et al. (2015; 2016) and Allen et al. (2020a) in a western US study on climate change effects on irrigation demands. An expected outcome of the use of normalized NCGDD is that the evolution of the K_{cb} curve vs. NCGDD for the period from planting (when NCGDD = 0.0) to effective full cover (when NCGDD = 1.0) follows a similar shape for many agricultural crops, as illustrated in Figure 1. This outcome is due to similar development of leaf area and ground cover and, therefore, K_{cb}, in proportion to the relative accumulation of thermal units.

Establishing K_{cb} curves using fraction of cover and vegetation indices.

In the absence of K_{cb} information for specific crops or for vegetation types having unusual row spacings or planting densities, estimates for K_{cb} may best be derived using observations or estimates of fraction of ground covered by vegetation. In general, $K_{cb\ mid}$ is less when plant densities or leaf areas are less than those for full ground cover. In those situations, conversion of net radiation to transpiration is less and more sensible heat, H, is produced. The estimation of K_{cb} from fraction of ground covered by vegetation (Allen and Pereira, 2009) is gaining use (Pereira et al., 2020) due to the strong and generally consistent relationships between fraction of ground cover and transpiration from agricultural vegetation. Estimates for ET_c using fraction of ground covered can provide more specific estimates than using a generalized K_{cb} from a published table. Full ground cover is often associated with the leaf area index, LAI, being more than about 3.0 (Ritchie and NeSmith, 1991).

To construct a K_{cb} curve from observed fraction of ground cover, the K_{cb} at midseason, $K_{cb\ mid}$, can be used to define the maximum K_{cb} value. The $K_{cb\ mid}$ value can be expressed as a linear proportion of the range between $K_{c\ min}$ and $K_{cb\ full}$ according to a density coefficient, K_d, (Allen and Pereira, 2009):

$$K_{cb\,mid} = K_{c\min} + K_d \left(K_{cb\,full} - K_{c\min} \right) \tag{3}$$

where $K_{cb\ mid}$ is the approximation for K_{cb} during the midseason period, $K_{cb\ full}$ is the expected basal K_{cb} during peak plant growth under conditions of nearly full ground cover (or LAI > 3). $K_{c\ min}$ is the minimum K_{cb} for bare soil ($K_{c\ min}$ ~ 0.15 under typical agricultural conditions and $K_{c\ min}$ ~ 0.0 to 0.15 for native vegetation, depending on rainfall frequency). The density coefficient K_d represents the relative and effective fraction of ground surface covered or shaded by vegetation. K_d can be estimated as a function of measured or estimated leaf area index (LAI) or as a function of fraction of ground covered by vegetation, adjusted according to plant height.

For tree crops that have grass or some other ground cover that can increase the overall K_{cb}, Eq. (3) can be modified to:

$$K_{cb\ mid} = K_{cb\ \mathrm{cover}} + K_{\mathrm{d}} \left[\max\left(K_{cb\ \mathrm{full}} - K_{cb\ \mathrm{cover}}, \frac{K_{\mathrm{cb\ full}} - K_{cb\ \mathrm{cover}}}{2} \right) \right] \tag{4}$$

where $K_{cb\ \mathrm{cover}}$ is the K_{cb} of any ground cover in the absence of overhead foliage. The second term of the max function reduces the estimate for $K_{cb\ mid}$ by half the difference between $K_{cb\ \mathrm{full}}$ and $K_{cb\ \mathrm{cover}}$ when this difference is negative. This accounts for impacts of shading of the surface by vegetation having a K_{cb} that is lower than that of the surface cover, due to differences in stomatal conductance. Eq. (3) and (4) can be applied to estimate K_{cb} during other periods besides the midseason.

Eq. (4) can similarly be applied to estimate a mean K_{cm} for any period with less than full vegetative cover by accounting for the effect of evaporation from predominately exposed areas of soil among the vegetation, similar to what is done in the dual $K_{cb} + K_e$ approach:

$$K_{cm} = K_{\mathrm{soil}} + K_{\mathrm{d}} \left[\max\left(K_{cb\ \mathrm{full}} - K_{\mathrm{soil}}, \frac{K_{cb\ \mathrm{full}} - K_{\mathrm{soil}}}{2} \right) \right] \tag{5}$$

where K_{soil} represents the average K_c from the nonvegetated (exposed) portion of the surface. The value for K_{soil} reflects the effect of wetting frequency, soil type, and relative ET rate (i.e., ET_{ref}) during the same period as K_d and $K_{cb\ full}$. The K_{cm} represents an average K_c value that considers the mean impact of evaporation from soil. K_{cm} can be used to represent the midseason or other period as defined by K_d, K_{cm}, and $K_{cb\ full}$.

For large areas of vegetation (greater than about 500 m^2), $K_{cb\ \mathrm{full}}$ for use with ET_o can be approximated as a function of mean plant height and adjusted for climate similar to the $K_{cb\ mid}$ parameter, following Allen et al. (1998):

$$(\text{for } ET_o) \ \ldots\ldots\ K_{cb\,\mathrm{full}} = \min\left(1.0 + 0.1h,\ 1.20\right) + \left[0.04(u_2 - 2) - 0.004(RH_{\min} - 45)\right]\left(\frac{h}{3}\right)^{0.3} \tag{6}$$

where h is mean maximum plant height in m, u_2 is the mean value for wind speed at 2-m height during the mid-season in m s^{-1}, and RH_{min} is the mean value for minimum daily relative humidity during the mid-season in %. For use with alfalfa reference ET_r, $K_{cb\ full}$ can be approximated for crops as

$$(\text{for } ET_r) \text{ ....} \ K_{cb\,\text{full}} = \min\left(0.8 + 0.1h,\ 1.0\right) \tag{7}$$

The climatic correction is not required for $K_{cb\,full}$ for use with ET_r because the aerodynamic and canopy characteristics of the alfalfa reference crop cause ET_r to approximate near maximum ET under a broad range of climates.

The value $K_{cb\,full}$ represents a general upper limit on $K_{cb\,mid}$ for tall vegetation having full ground cover and LAI > 3 under full water supply. Eqs. (6) and (7) produce general approximations for the increase in $K_{cb\,full}$ with plant height and climate. The estimate may need adjustment downward if the vegetation exhibits more stomatal control on transpiration than is typical for agricultural crops, for example, for some types of trees or natural vegetation (Allen et al., 1998; Allen and Pereira, 2009).

When LAI is measured or can be approximated, K_d can be approximated (Allen et al. 1998) as

$$K_d = \left(1 - e^{[-0.7\,LAI]}\right) \tag{8}$$

LAI is defined as the area of leaves per area of ground surface averaged over a large area with units of $m^2\ m^{-2}$. Only one side of green healthy leaves that are active in vapor transfer is considered. The relationship in Eq. (8) is similar to one used by Ritchie (1974).

When the fraction of ground surface covered by vegetation is observed or estimated, the K_d can be estimated as a function of $f_{c\,eff}$ and vegetation height (Allen and Pereira, 2009):

$$K_d = \min\left[1, M_L\, f_{c eff}, f_{c eff}^{\left(\frac{1}{1+h}\right)}\right] \tag{9}$$

where M_L is a multiplier on $f_{c\,eff}$ describing the effect of canopy conductance on maximum relative ET per fraction of ground shaded (1.5–-2.0), $f_{c\,eff}$ is the effective fraction of ground covered or shaded by vegetation (0.01–1) near solar noon, and h is the mean height of the vegetation in m. The M_L multiplier on $f_{c\,eff}$ in Eq. (9) imposes an upper limit on the relative magnitude of transpiration per unit of ground area as represented by $f_{c\,eff}$ (Allen et al. 1998) and is expected to range from 1.5 to 2.0, depending on the canopy density, thickness, and maximum conductance. Parameter M_L is an attempt to simulate the physical limits imposed on water flux through the plant root, stem, and leaf systems (Allen and Pereira, 2009). The value for M_L can be modified to fit the specific vegetation. Equations 3-7 and 9 have been adopted in the SIMS model by Melton et al. (2012) and Johnson et al. (2016) to provide spatial estimation of K_{cb} at 30 m Landsat satellite scale by estimating f_c from normalized difference vegetation index (NDVI). The height parameter, h, increases the estimate for K_d and therefore K_{cb} to account for the influence of taller vegetation height on intercepting solar radiation and on increasing aerodynamic roughness of vegetation and therefore vapor exchange into the boundary layer.

The use of a skin evaporation layer for K_e from light wetting events

A recent development in the dual K_{cb} methodology has been the improvement in estimation of K_e by including immediate stage 1 evaporation from the soil "skin" following light wetting events. The FAO-56 model for evaporation from bare soil, expressed as K_e, has become widely applied for both bare soil conditions and as a part of the dual K_c method via Eq. 1. The dual methodology has had more than 450 citations in Google Scholar (https://scholar.google.com). The K_e model conducts an hourly or daily soil water balance for a 100 to 150 mm thick 'slab' and divides the evaporation process into stage 1 (wet) and stage 2 (drying surface) processes. As illustrated in Figure 3, the K_e model can be effective in simulating evaporation associated with soil wetting events associated with precipitation and irrigation. The "skin" enhancement to the FAO-56 K_e model (Allen, 2011; ASCE 2016) conducts an additional water balance for the upper soil 'skin' so that small additions of water from sprinkling or precipitation are evaporated off relatively quickly as flash events, rather than mixed into the entire slab as assumed in the original 1998 model. The skin enhancement provides good agreement with measured evaporation and with simulations of K_e by the Hydrus model (Šimunek et al. 2005; Allen, 2011).

Ranade (2010) constructed an ArcMAP based K_e model that created gridded precipitation and reference ET data from point weather measurements and then applied the FAO-56 K_e model to produce gridded K_e that was used to adjust Landsat-based ET maps from METRIC (Kjaersgaard et al., 2011). Kilic and Kamble applied the FAO-56 K_e model on the Google Earth Engine to produce gridded K_e maps on a monthly basis for the continental United States (Kilic et al., 2015).

Winter time K_c *and importance to hydrologic studies*

Nongrowing periods are defined as periods during which no agricultural crop has been planted. In temperate climates, nongrowing periods may include periods of frost and continuously frozen conditions. Traditionally, ET during nongrowing periods has been ignored during determination of irrigation water requirements and ET for water rights. However, estimation of ET during nongrowing periods can be important in annual water balances used in hydrologic studies and for estimation of accruals to soil water from precipitation during nongrowing seasons. Procedures for estimating ET during nongrowing periods have evolved over the past 25 years to the point of providing relatively dependable estimates for ET that incorporate a practical combination of physically based and empirical relationships.

The type and condition of the ground surface during nongrowing periods dictate the range expected for K_c. Current constructs for applying crop coefficient procedures during nongrowing periods are described in ASCE (2016). The constructs use Eq. (3)-(9) with relatively straightforward recommendations on their employment. When the surface is bare soil, then

K_c will be similar to values estimated for K_{soil} or K_e. When dead or dormant vegetation, or some type of organic mulch or crop residue, cover the surface, then K_c will be similar to that for agriculture having a surface mulch. When weed growth or "volunteer" plants cover the surface, then K_c will vary according to the green leaf area or fraction of ground covered by the vegetation, as estimated by Eq. (5) using K_d from Eq. (8) or (9), and by the availability of soil water. When the surface is snow covered or frozen, then K_c is difficult to estimate and a low, constant value for K_c may have to be assumed (Allen et al., 2020a).

Bare Soil. When the ground is mostly bare following harvest or removal of vegetation, the frequency and amount of precipitation will strongly influence K_c. In the single K_c procedure, the K_{cm} for bare soil can be calculated as $K_{cm} = K_{soil}$. Martin and Gilley (1993) and Allen et al. (1998) recommended this approach, and Snyder and Eching (2005) used a similar approach in their LIMP software (http://biomet.ucdavis.edu/irrigation_scheduling/LIMP/LIMP.htm) to estimate a K_{cm} during winter that is then melded with a K_{cm} curve for the growing season. When a daily soil water balance can be applied, the user may elect to apply the dual or basal K_{cb} approach as recommended by Allen et al. (1998) and ASCE (2016).

Surface Covered with Dead Vegetation. Stubbles and mulches reduce soil evaporation by providing a mechanical barrier to aerodynamic forces and shielding the soil surface from solar radiation. Mulches also reduce the connection between liquid or vapor in the soil and the air above (Burt et al., 2005a). Burt et al. (2005a) described studies of evaporation experiments from organically mulched soil covers and reported a 20% reduction in E from a no-till standing wheat stubble as compared with conventional tillage in North Dakota, a 40% reduction in E from standing wheat stubble in cotton in Texas, and a nearly 50% reduction in E from soil covered with spread straw relative to bare soil in Nebraska. They noted that soil surface mulches are less effective at reducing soil evaporation under dryland conditions where longer periods for drying between wetting events can slowly deplete soil water as compared with conditions under more frequent wetting with irrigation. Allen et al. (1998) suggested reducing the value for K_{soil} by about 5% for each 10% of soil surface that is effectively covered by organic mulch.

Surface Covered with Live Vegetation. During frost-free periods following harvest, weeds may germinate and grow. This vegetation extracts water from storage within the soil profile and from any rainfall. In addition, crop seed lost during harvest may germinate following rainfall events and add to the ground cover. The amount of ground surface covered by vegetation will depend on the severity of weed infestation, the density of the volunteer crop, the frequency and extent of soil tillage, the availability of soil water or rain, and any damage by frost. The value for K_{cb} during the nongrowing period can be estimated over time according to the amount of vegetation covering the surface using Eqs. (5)–(9) or from remote sensing images by way of a vegetation index (Melton et al., 2012; Johnson et al., 2016).

The K_c or K_{cb} for vegetation during the nongrowing period should be limited by the amount of soil water available to supply evapotranspiration to satisfy the law of conservation of mass. Under all conditions, the integration of K_c times ET_{ref} over the course of the nongrowing period should not exceed the sum of precipitation occurring during the period plus any residual soil water remaining in the root zone after harvest that can be subsequently depleted by vegetation plus any upward flow from a shallow saturated system. The root zone in this case is the root zone of the weeds or volunteer crop. An hourly or daily soil water balance may provide the best estimate of soil water–induced stress and associated reductions in K_c and ET_c. due to its ability to account for sequencing of wetting and drying events and intervals and any movement of water to below the root zone or evaporating layer.

Tasumi et al. (2005) and Allen et al. (2007a) sampled populations of K_c in south central Idaho for major crop types using a Landsat satellite-based surface energy balance. Large variances in distributions of K_c occurred during March and April and reflected the large variation in development of and wetness of winter wheat fields coming out of winter dormancy. Additional variation in K_c among fields of wheat occurred following harvest of the crops, where variation averaged about 0.20. Causes for the variation included the timing of senescence of the wheat field or variety, the amount of post-harvest vegetation present in the form of weeds, nursed alfalfa, or volunteer wheat, and variation in irrigation of fields following harvest, coupled with cultivation. Variances of distributions of K_c during the period of peak K_c were small because nearly all fields were at or near effective full cover so that K_c values clustered closely about 1.0 when used with the alfalfa reference ET_r.

*Frozen and Snow-Covered Surfaces***.** When the ground surface is snow covered or frozen, any vegetation will be largely nonresponsive and will not contribute directly to ET_c. In these situations, ET_c will be closely related to the availability of free water at the surface and to the albedo of the surface. The albedo of snow-covered surfaces can range from 0.40 for old, dirty snow cover to 0.90 for fresh, dry snow. Therefore, the ET_c for snow cover will be less than ET_{ref}, as 25-85% less shortwave energy is available. In addition, some energy must be used to melt the snow before evaporation, besides energy consumed in melting snow that seeps into the snowpack. Under conditions of snow cover where the surface of the snow does not have a liquid film, the saturation vapor pressure at air temperature used in the vapor pressure deficit calculation in the Penman-Monteith reference equation should be computed for over ice rather than water (ASCE, 2016).

The use of ET_{ref} under winter conditions is of limited value, as the assumption of conditions sustaining a green grass or alfalfa cover during frozen periods is violated. It is even possible to obtain negative values for ET_{ref} on some winter days when the longwave radiation from the surface is large and the vapor pressure deficit is small. Under these conditions, net condensation of water from the atmosphere is possible, which corresponds to negative evaporation. Given the limited utility of using ET_{ref} under snow-covered or frozen conditions, use of a single average value may be justified to estimate ET_c. Wright (1993) measured ET_c averaging 1 mm d^{-1} over nongrowing season periods at Kimberly, Idaho that were six months long (1 October to 30 March). The latitude of Kimberly is 42°N, and the elevation is about 1,200 m. Over the six-year study period, the ground was at least 50% covered by snow for 25% of the time from 1 October to 30 March. The ground, when exposed, was frozen about 50% of the time. The K_c averaged 0.25 during periods when the soil was not frozen but where frosts occurred (October and early November). When the ground had 50% or greater snow cover, ET_c averaged only 0.4 mm d^{-1}. Wright found that over the six-month nongrowing period, total cumulative ET_c exceeded precipitation by about 50 mm, indicating a drying soil condition.

The K_{cm} measured by Wright (1993) and converted to the standardized Penman-Monteith alfalfa reference ET (ET_r) basis averaged about 0.45 during the October-December period over years 1985-1991 for dormant fescue grass cover and for nongrass covers including tilled soil. Even though these values for K_{cm} are high due to the relative wetness of the surface during the nongrowing periods, the total ET rates were low due to low values for ET_r during these periods. Allen (1996b), found ET_c to vary widely with soil surface wetness and air temperature during winter months near Logan, UT for grass pasture. The average K_c from November to March was 0.5 for days having no snow cover. For days with snow cover, ET_c ranged from 0 to 1.5 mm d^{-1}.

A daily soil water balance using the dual crop coefficient approach may improve accuracy in estimating ET_c under freezing and snow-covered conditions. For example, Allen et al., (2020a) applied a daily model for evaporation during winter that included a snow melt estimate. In their implementation of a dual crop coefficient, a daily water balance was conducted for the top soil slab that contributes to evaporation (Allen et al., 1998; Allen, 2011). The daily estimate for K_c was reduced according to available soil water. In addition to the limited validity of the concept of ET_{ref} under frozen or snow-covered conditions, the evaporation coefficient, K_e, may have low values when the ground surface is frozen, as the water in a frozen state is less available. When the basis for K_c during nongrowing periods is the ASCE PM alfalfa reference ET_r, where the crop is a hypothetical potential reference representing 0.5-m tall green alfalfa, under even wet conditions, the K_c during winter time is not expected to reach 1.0 over extended periods of time because vegetation may be frozen, cold stressed, or dormant.

Somewhat complex models for estimating ET_c under nongrowing season conditions, snow cover, and freezing are available in the literature and can be consulted and perhaps applied when precise estimates for ET_c are required, for example in Flerchinger (1991), Flerchinger et al. (1996), and Saxton and Willey (2005). Allen and Robison (2007) and Allen et al., (2020a; ASCE, 2016) applied the concepts described in the previous section to estimate daily ET for all days of the year including winter. They defined the nongrowing season period as beginning when a K_{cb} curve representing the growing cycle for a specific crop ended or when a killing frost occurred. They defined the nongrowing season as ending at greenup or planting of the same crop the following year (or October 1 in the case of winter wheat). A basal K_{cb} of 0.1 was used for bare soil conditions during nongrowing season periods, for surfaces covered with some amount of mulch, and for dormant turf/sod systems. K_{cb} represented conditions when these surfaces had a dry soil surface but had sufficient moisture at depth to supply some diffusive evaporation. The evaporation (K_e) component was estimated separately in the daily soil water balance, where $K_{c\ max}$ during the nongrowing period was 0.9 for bare soil, 0.85 for mulched surfaces, and 0.8 for dormant grass cover. The lower value for grass accounted for the insulative effects of grass and its higher albedo. An effective "rooting zone" of 0.10 m was used during the nongrowing season for the fraction of surface under a cover. For all surfaces, a daily soil water balance was calculated and a stress coefficient was applied when soil water content of the upper 0.10 m dropped below a critical value. This caused actual K_c to fall below K_{cb} when both the ground surface and subsurface soil were dry. All land use types, including agricultural, landscape, horticultural, and natural vegetation, were assigned one of the three winter cover conditions (dormant grass, bare soil, or mulch classes) for estimating evaporation losses during winter. Allen and Robison (2007) and Allen et al., (2020a) described functions for estimating sublimation from snow.

The use of alfalfa vs. grass references and 24-hour vs. hourly calculation timesteps

The standardized PM method, applied daily, is considered by ASCE (2005; 2016) to be accurate and dependable for application during growing periods. The 24-hour calculation timestep was, in fact, used during the ASCE standardization work to guide the selection of surface resistance values for hourly time step applications. The daily time step, however, may not accurately estimate reference ET during freezing winter and other nongrowing season periods, where conditions represented by the reference crop do not physically exist (surface resistance of 45 s m^{-1} for ET_{rs} and 70 s m^{-1} for ET_{os} over a 24-h period). The hourly calculation time step, because it keeps radiation and aerodynamic parameters synchronized in time, is considered to be more dependable and accurate in simulating the ET conditions represented by the standardized definitions, especially under conditions where wind speed, solar radiation, and vapor pressure deficit are not in proximate time synchronization during the day, such as during winter. The use of hourly time steps enables a more accurate energy balance process calculation than 24-h time steps during times of the year when day length is short. During these times, some of the compensating assumptions in the procedures for applying the combination method on a 24-h time step may break down. For example, in the 24-h net radiation calculation, the short wave component may occur over an eight-hour period, whereas the incoming and outgoing long-wave radiation component occurs over the entire 24-hour interval. As a result, hourly calculations of reference ET are encouraged by ASCE (2005; 2016), especially during winter. In addition, the grass reference ET_o may be preferred over alfalfa ET_r during wintertime, especially if 24-hour calculation timesteps are employed, since ET_o is a somewhat 'softer' reference and more likely mimics surface conditions found during winter than does alfalfa.

Application of ET equations over only daytime periods (i.e., ignoring calculations during nighttime) is discouraged. This practice ignores any ET that may occur during nighttime, which can be as much as 15% of 24-h ET during the growing season in arid and semiarid climates (Tolk et al., 2006). In addition, application of the combination or energy balance equation solely for a daytime period requires estimation of soil heat flux, G, which cannot be assumed to be zero as it generally can for 24-h calculation time steps.

Current Directions

Use of gridded weather data

Over the past 10 to 20 years, the advent of gridded historical weather data derived from sophisticated land data assimilation systems (LDAS) operated by NOAA's National Centers for Environmental Prediction (NCEP) and the National Science Foundation sponsored National Center for Atmospheric Research (NCAR) has provided an alternative data source to the traditional use of point-based weather station data for estimating reference ET. LDAS systems are operated for purposes of weather research and weather and climate forecasting. The LDAS systems assimilate electronically available weather data from point weather sites around the globe and couple those data with land process (soil and vegetation water balance) models and with atmospheric models to extend the point data and create weather circulation patterns and associated gridded weather data sets that are traceable to the original point measurements. Data products include the 30+ year (1979-present) North American Land Data Assimilation System (NLDAS) retrospective forcings (Mitchell et al., 2004) having 1/8 degree resolution (~ 12 km x 12 km), the Climate Forecast System version 2 (CFSV2) of NOAA (https://www.ncdc.noaa.gov/data-access/model-data/model-datasets/climate-forecast-system-version2-cfsv2), hourly from 2011 to present at 45 km; and Modern-Era Retrospective analysis for Research and Applications, Version 2 (MERRA-2) by NASA (https://gmao.gsfc.nasa.gov/reanalysis/MERRA-2/) at about 50 km resolution.

NLDAS phase 2 retrospective forcings (NDAS-2) contain daily precipitation, solar radiation, and 2m reference height temperature and humidity, and 10m reference height windspeed (http://www.emc.ncep.noaa.gov/mmb/nldas/). Model-based NLDAS forcings of temperature, humidity, and windspeed are derived from spatially and temporally interpolated NCEP North American Regional Reanalysis (NARR) data. Observation-based NLDAS forcings include GOES based solar radiation, and gauge- and NEXRAD-based precipitation.

Other nonforecast data bases include the 24-hour PRISM data set of Oregon State University (http://www.prism.oregonstate.edu/) that, in addition to containing lapse-adjusted precipitation at 1 and 4 km scales, now includes gridded air temperature and humidity data, and the DAYMET daily gridded data at 1 km resolution containing surfaces of minimum and maximum temperature, precipitation, vapor pressure, radiation, snow water equivalent, and day length (https://daymet.ornl.gov/overview). The GridMET system (http://www.climatologylab.org/gridmet.html) has become a popular gridded daily weather system that provides high spatial resolution (~4-km) daily surface fields of temperature, precipitation, winds, humidity and radiation across the contiguous United States from 1979 to present. GridMET blends the high-resolution spatial data from PRISM with the high temporal resolution data from the National Land Data Assimilation System (NLDAS) to produce spatially and temporally continuous fields that lend themselves to additional land surface modeling (Abatzoglou, 2013).

Most of the gridded weather data sets can be downloaded automatically from sources using Python-style scripts, brought into geospatial processing structures such as ArcMAP or Python-GDAL scripts and processed to reference ET. Some grids including GridMET, NLDAS and CFSV2 are available in near-real time on the Google Earth Engine.

Some previous applications of reference ET computations made with gridded LDAS types of data systems include Senay et al. (2008), who applied the FAO-56 based PM reference ET method to 1.0-degree LDAS data for the globe. They compared against ET_{ref} derived from the California Irrigation Water Management Information System (CIMIS) by matching grid points and found relatively good correspondence. Similar studies were done by Hidalgo et al. (2005) for California, and in Florida by Said et al., (2006). The National Weather Service produces an Experimental Forecast Reference Evapotranspiration (FRET) grid for much of the USA via regional weather forecast centers (https://www.weather.gov/cae/fretinfo.html). The grass reference ET_o from FRET is available in real time and as a six day forecast. The forecast data are useful in guiding irrigation scheduling.

The ET_{ref} applications in the preceding paragraph do not tend to evaluate nor mitigate for the impacts of dryness of weather sites assimilated into the LDAS data sets on reference ET calculated from those data sets. Causes of dryness of LDAS data sets include the usual lack of irrigation inputs into their soil water balances and subsequent under-simulation of ET and humidification of the near-surface boundary layer. The resulting dryness of the LDAS data sets can have a substantial impact on subsequent reference ET estimates. This impact is discussed in the next section. The impact can overstate computed ET_{ref} by as much as 20 to 30%, (Blankenau et al., 2020), substantially reducing the value and adequacy of the LDAS-based ET_{ref} estimates for irrigation planning, design and management and hydrologic studies.

Biases in gridded data

The gridded data sets typically represent 'ambient' environments, which in the western US are largely dry, nonirrigated environments. As a result, the simulated near surface weather data, although valuable for describing the natural, ambient conditions in the absence of human-caused irrigation, can cause irrigation water requirements and ET to be overestimated by as much as 20 to 30% (Blankenau et al., 2020). In the past, empirical methods have been developed to adjust arid air temperature downward and, in some cases, adjust arid vapor pressure upward (Jensen et al., 1997; Allen et al., 1998; Temesgen et al., 1999). Recently research has developed theoretical boundary layer procedures to "condition" gridded data sets to better reflect weather data that would have been collected in an area under well-watered (irrigated, or 'reference') conditions (Allen et al., 2020b). Those adjustments modify profiles for T, humidity and wind speed in the near surface atmospheric boundary-layer by establishing the ambient boundary layer profiles for air temperature, humidity and wind speed, and then replacing dry surfaces with well-watered reference surfaces and re-extrapolating those profiles using energy-balance equations to a blending layer at 50 m height. The boundary layer method transforms gridded (hourly, 3-hourly and daily) NARR and NLDAS weather data into 'conditioned' weather data series that reflect properties of the near surface boundary layer when that boundary layer were to exist over an extensive well-watered reference type of vegetation. The resulting conditioned data are generally cooler and more humid than the original data set, assuming that the original data were collected over, and are representative of, extensive, dry surfaces representing the original ambient conditions. The conditioned weather data are more suitable to use to compute gridded reference evapotranspiration representing the special and specific equilibrium conditions that are experienced over irrigated surfaces. The conditioned ET_{ref} estimates incorporate the dampening feedback brought into the near surface atmospheric boundary layer by the presence of vapor flux supported by irrigation and that provides a negative, dampening feedback to the ET process.

Figures 4 and 5 show 3-hourly air temperature and 3-hourly vapor pressure for a North America Regional ReAnalysis (NARR) data set, which is similar to the NLDAS data set, for a grid cell located near Twin Falls, Idaho during a period during May, 2008. The data are compared against measured air temperature and vapor pressure from the Twin Falls Agrimet station that is an electronic, automated weather station that is located in an irrigated agricultural location. While there is close correspondence between the two data sets, which is a very positive indication of good assimilation of general weather data on a local scale, the NARR temperature overstated the Agrimet air temperature by up to 5 °C, and the vapor pressure (i.e., near surface water vapor content) was understated by one-half, due to the impact of assimilation of weather data in the NARR (and NLDAS) gridded data sets from dry (airport, etc.) stations. These types of outcomes are common, and again, cause overestimation of ET_{ref} by as much as 20 to 25% by ignoring the influence of conditioning of the equilibrium boundary layer (EBL) by evaporative cooling that occurs over irrigated agriculture (Jacobs and deBruin 1992, Brown, 2001; ASCE, 2005; Allen, et al., 2020b; Blankenau et al., 2020).

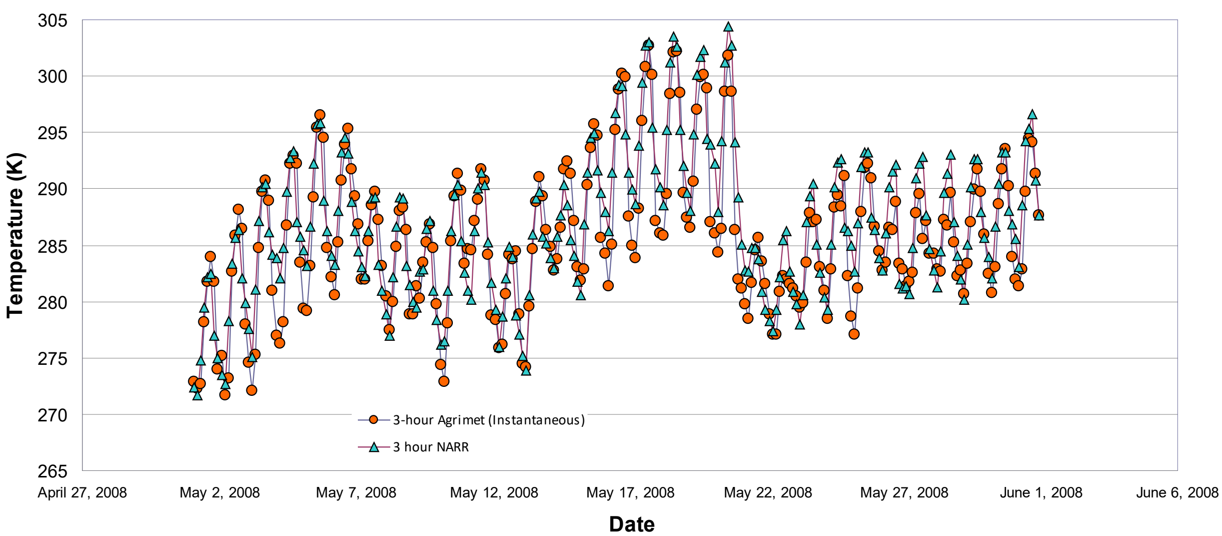

Figure 4. Three-hourly air temperature data from the North American Regional Reanalysis data set for a grid cell over Kimberly, Idaho, during May 2008, compared with measured air temperature collected at the USBR Agrimet weather station (TWFI) located near Kimberly. The Agrimet station is located over irrigated grass and generally runs cooler than the NARR data that is impacted by using ambient data from nonirrigated weather sources.

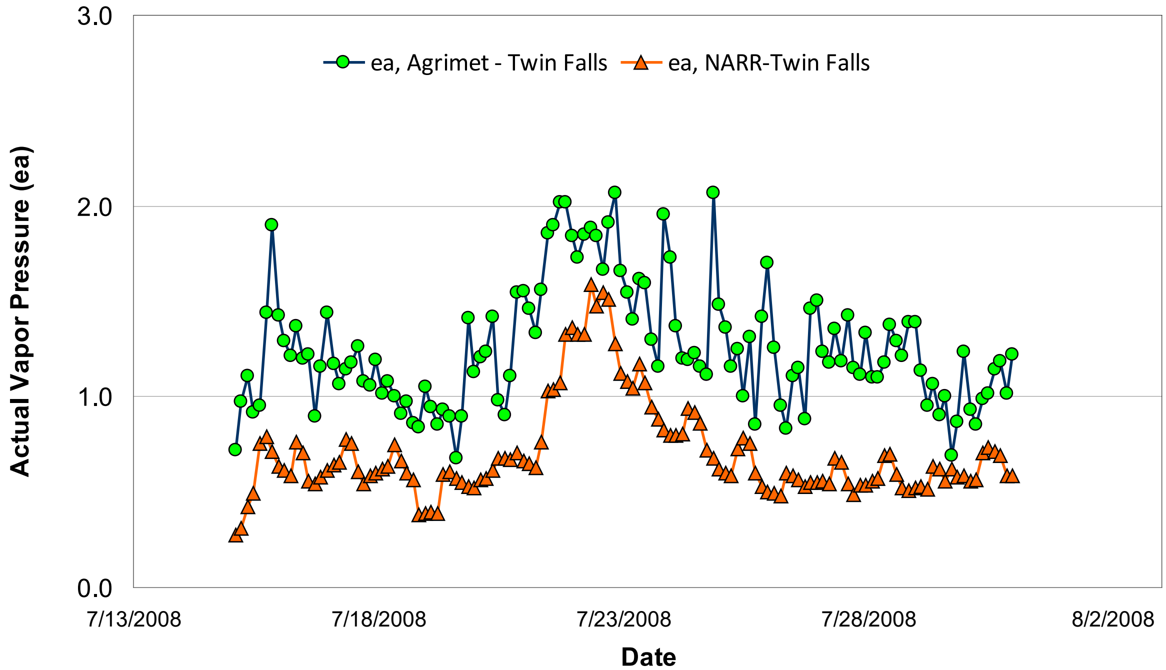

Figure 5. Three-hourly vapor pressure data from NARR over Kimberly, ID, during May 2008, compared with measurements at the USBR Agrimet weather station (TWFI) near Kimberly. The Agrimet station is over irrigated grass and has *double the humidity* than the NARR data that is impacted by ambient data from nonirrigated weather sources.

Figure 6 shows daily values for daily maximum air temperature for the 'reference' T_{max} at Kimberly, ID (over irrigated alfalfa) and original desert T_{max} ('Desert") as measured (ambient) during July and August 2009, and showing the results where the 'Desert' data were conditioned (adjusted) to 'reference' T_{max} using the boundary-layer based adjustment by Allen et al. (2020b). The adjustments are, on average, good in matching Kimberly data, with some variation in the effectiveness of the conditioning from day to day. Average adjustment to the temperature data was about 2^{o}C. Very low values were caused by numerical instability in Monin-Obhukov computations.

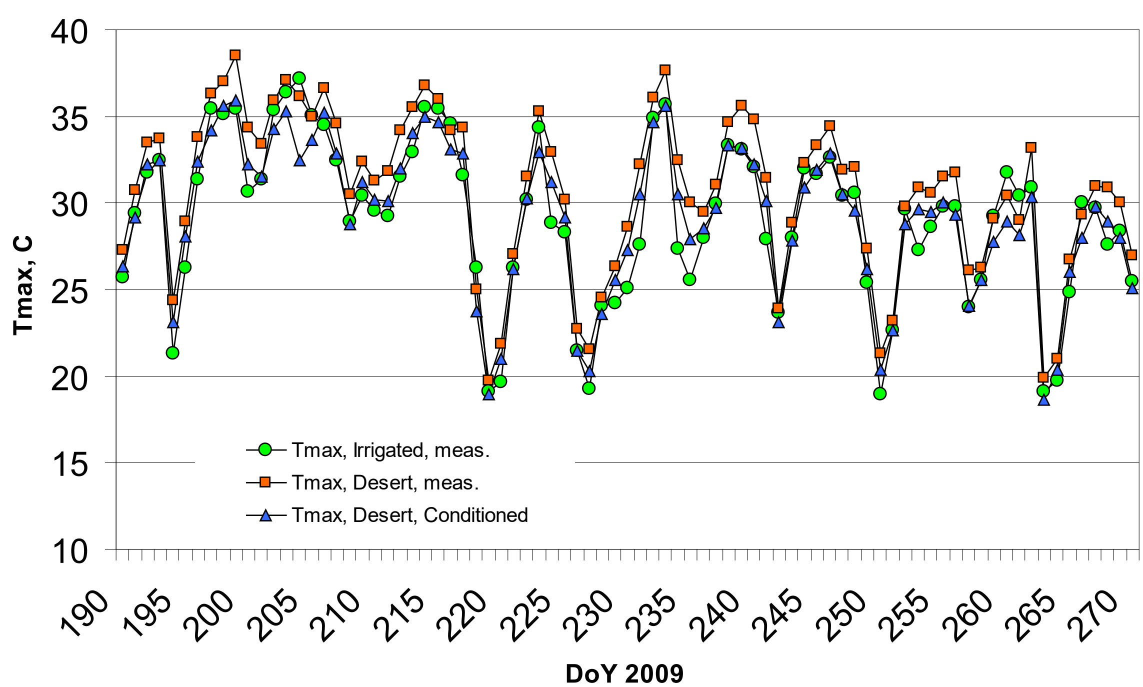

Figure 6. 'Reference' T_{max} at Kimberly, ID (over irrigated alfalfa) and original desert T_{max} 80 km west of Kimberly as measured (ambient), and the results after conditioning the desert data to a 'reference' T_{max}.

Vapor pressure measured at the Kimberly and Desert locations and the Desert data conditioned into an equilibrium, reference condition is shown in Figure 7. Similar to the previous comparison against NARR data in Figure 5, vapor content over the irrigated Kimberly site was nearly double that measured over the measurements in desert, which represents an ambient condition for the southern Idaho region. The conditioning of the ambient data brought the vapor content (expressed as vapor pressure) close to that measured over the irrigated surface.

Wind speed measured at the Kimberly and Desert locations is shown in Figure 8, along with wind speed based on the conditioned Desert data. Wind speed was about 20% stronger over the desert site than over the irrigated site due to lower aerodynamic roughness at the desert and due to impacts of large sensible heat flux and buoyancy over the desert that fostered downward entrainment of higher velocity air from aloft toward the warmer surface. The entrainment process, which also produces advection of energy to irrigated fields, was moderated over the irrigated site by the lower sensible heat flux and reduced buoyancy at Kimberly. The conditioning process tended to reduce the wind speed observed at the Desert site by nearly 20%.

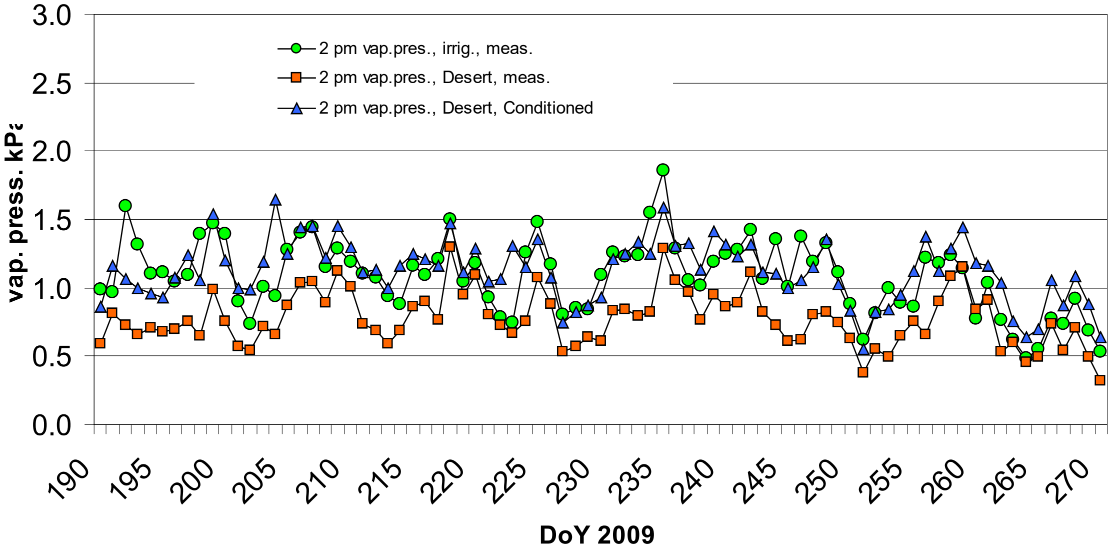

Figure 7. 'Reference' vapor pressure at Kimberly (over alfalfa) and original Desert vapor pressure as measured (ambient), and results from conditioning data measured at 2 pm. The adjustments are, on average, good in matching Kimberly data, but vary from day to day in accuracy.

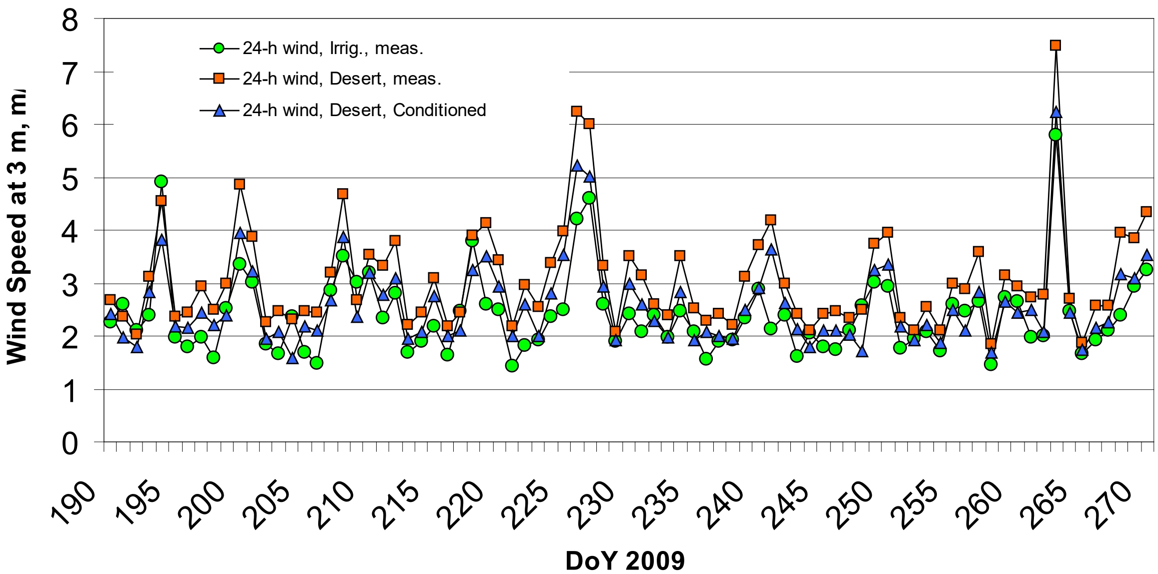

Figure 8. Wind speed measured at the southern Idaho Desert site vs. that measured at the Kimberly, Idaho irrigated site and vs. conditioned Desert data. The conditioning brought ambient Desert wind speed towards that measured at the irrigated site for a majority of days, with dampening of wind speed by about 20%.

All three weather parameters (air temperature, humidity, wind speed) impacted by the conditioning process were adjusted in directions that reduced the estimates for grass reference ET_o. Figure 9 shows reference ET estimated for midafternoon using the Desert weather data before and after conditioning. The ET fluxes, expressed as latent energy, reduced by about 10% following the conditioning. Figure 10 shows 24-hour (daily) grass reference ET_o in mm d^{-1} computed from the weather data collected at the Desert site using ambient measured T_{max}, T_{min}, vapor pressure, solar radiation and wind speed, and as also calculated from conditioned 'reference' T_{max}, vapor pressure, and wind speed. The calculations are compared to ET_o calculated from weather data measured 80 km east near Kimberly, Idaho over alfalfa. The impact of the adjustments on a daily basis was substantial, averaging 10 to 20% reduction in estimated ET_o, and the conditioned ET_o were in good agreement with the 'target' ET_o computed from the Kimberly data.

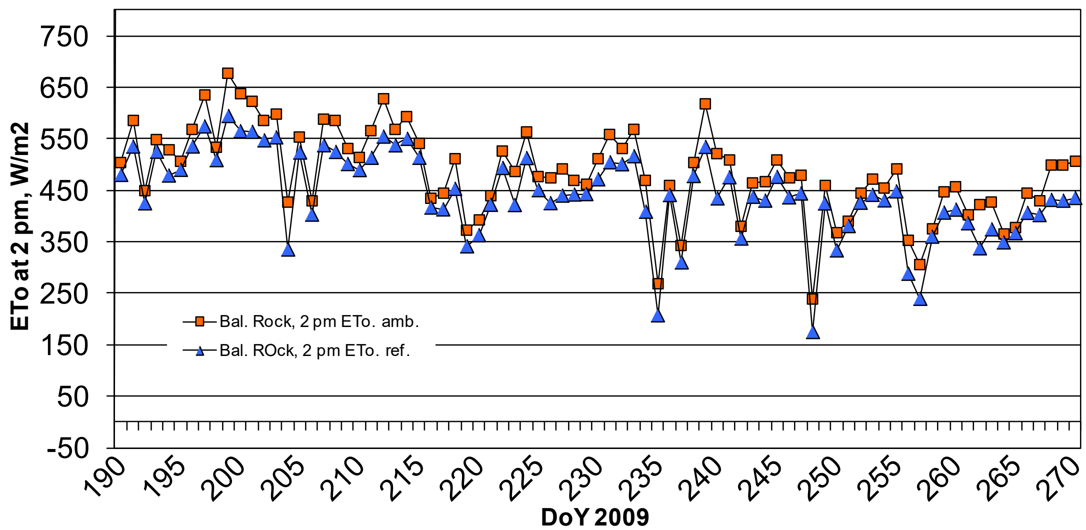

Figure 9. Grass reference ET_o in Wm^{-2}, computed at 2 pm at the Desert (Balanced Rock – amb.) site using original desert T_{max}, v.p. and wind speed as measured (ambient), and results from computing ET_o after conditioning the weather data to a reference (Bal. Rock, 2 pm ETo ref.). The impact of the adjustments was moderate, averaging about 10% reduction in estimated midafternoon ET_o.

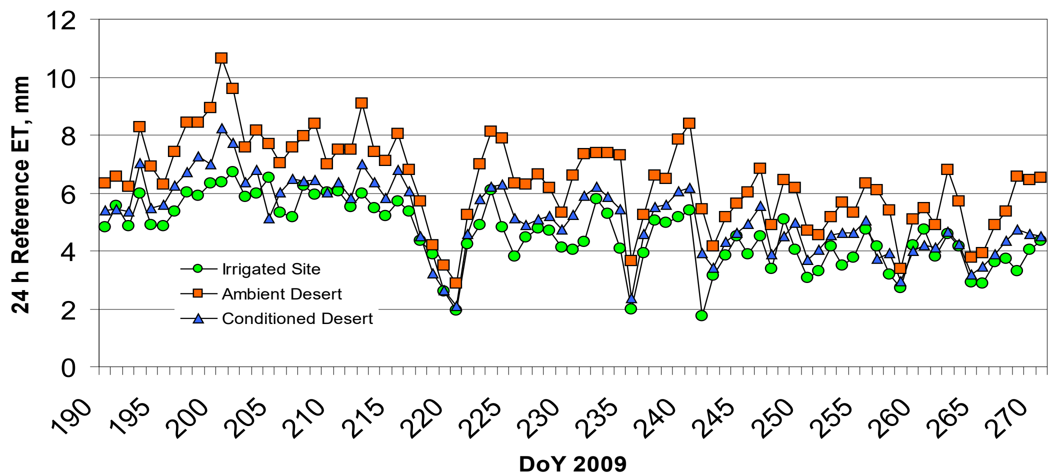

Figure 10. 24-hour (daily) grass reference ET_o in mm d^{-1} computed from weather data collected at the Desert site using ambient measured T_{max}, T_{min}, v.p., solar radiation and wind speed, and calculated from conditioned T_{max}, v.p., and wind speed from the Desert site. The ET_o calculations are compared to ET_o calculated from weather data measured 80 km east near Kimberly over alfalfa.

In summary, the conditioning of gridded weather data to remove artifacts of aridity using theoretical boundary layer theory (Allen et al., 2020b) tends to remove a majority of aridty biases in the original data. It is possible that future gridded weather data sets as well as weather data measured at arid ground locations such as at western USA airports can be run through a conditioning process prior to their use to estimate reference ET that represents ET from the reference crop in a relatively well-watered (irrigated) setting. The result will be more accurate estimates of ET expected from irrigated environments.

Use of remote sensing of ET by energy balance to determine ET and crop coefficients

Spatial maps of ET at high resolution are of interest to agriculture, water resources and national security as an indicator of crop water deficits and depletions on scales of human activities and individual land holdings. Satellite-based ET products are now being used in water transfers, to enforce water regulations, to improve development and calibration of ground-water models, where ET is a needed input for estimating recharge, to manage streamflow for endangered species management, to estimate water consumption by invasive riparian and desert species, to estimate ground-water consumption from at-risk aquifers, for quantification of native American water rights, to assess impacts of land-use change on wetland health, and to monitor changes in water consumption as agricultural land is transformed into residential uses (Bastiaanssen et al., 2005; Allen et al., 2005; Tasumi et al., 2005; Allen et al. 2007b; Kalma et al., 2008; Singh and Kilic-Irmak, 2009; Kilic et al., 2012; French et al., 2015; Karimi and Bastiaanssen, 2015; Kilic et al., 2015). Spatial estimates of ET are essential components of general circulation and hydrologic models (Wigmosta et al., 1994; Betts et al., 1997; Overgaard et al., 2006) and spatial ET is used to infer soil moisture, a valuable input to weather and flood forecast models.

Most satellite-based methods for ET employ the energy balance equation because ET, comprised of the flux of vapor molecules into the air stream, is not readily visible by satellites, whereas, R_n, G and H, being radiative and thermal processes, can be detected or surmised from shortwave (solar) and thermal imagery. Once the latent heat flux, λE, is computed, the ET rate, expressed as a depth of water evaporated per unit time, for example, over a day, is calculated by dividing λE by the latent heat of vaporization, λ. λ represents that amount of energy required to complete the ET process. Remote sensing surface energy balance (RSSEB) methods take advantage of the physical fact that conversion of liquid water to the vapor form requires substantial amounts of energy. This conversion of liquid to vapor during the evaporation process involves the same physical requirements whether the process is transpiration of water from inside a plant leaf or evaporation of water from a wet soil surface. Approximately 2.4 million Joules (megajoules) of energy are required to evaporate one kilogram of water at room temperature. The energy source can be in the form of heat energy from the surrounding air (this is often termed “sensible heat” since it can be sensed with a thermometer) and the source can be the radiant energy from the sun and atmosphere in the form of photons contacting the evaporating surface. Energy from photons frees water molecules from a liquid to vapor state.

Satellite imagery has been found to provide a dependable basis for estimating ET (Allen et al., 2005; 2007b; Kalma et al., 2008; Kilic et al., 2012; French et al., 2015; Karimi and Bastiaanssen, 2015). The strong benefit of satellite-based models is the quantification of spatially variable ET over large areas. Remotely sensed ET can be transformed into K_c. Conversely, the K_c and reference ET concepts are useful for establishing upper limits on ET during application of energy balance methods. In addition, the fraction of reference ET, ET_rF, which is essentially equivalent to K_c, is often used to interpolate ET estimates between satellite over pass times (Allen et al., 2007a).

Figure 11 shows a sampling of three cropped fields near Boise, Idaho during year 2015 in the form of ET_rF computed for each date of a Landsat overpass. ET_rF was produced by the METRIC surface energy balance model (Allen et al., 2007a) and was interpolated between overpass dates using a dampened cubic spline to mimic expected phenological evolution with time. The alfalfa reference was used as the basis for calculating ET_rF. Effects of late season ET following harvest of winter wheat due to rain events illustrates the utility of thermal-based remote sensing in detecting off-season ET related to precipitation.

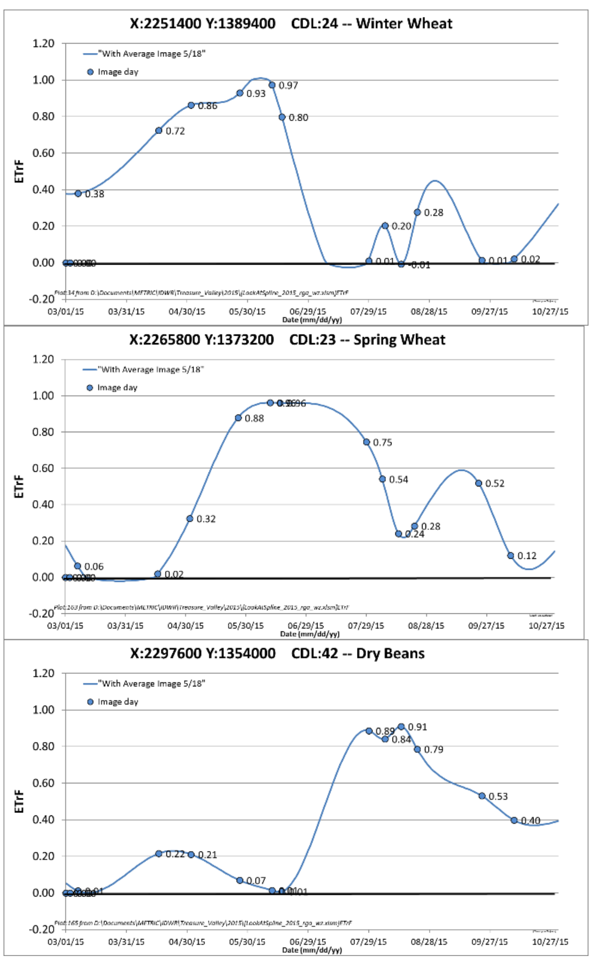

Figure 11. Sampled ET_rF (equivalent to actual K_c) for three cropped fields near Boise, Idaho during 2015 as produced by the METRIC remote sensing energy balance model, shown as symbols. The curved line represents splined interpolation of daily ET_rF between Landsat satellite overpass dates. X and Y locations are in meters for the Idaho Trans-Mercator. ‘CDL’ is the cropland data layer identification.

Satellite-based remote sensing has enabled the estimation of ET from large populations of individual fields (Tasumi et al.

2005) and has supported field-specific management of water systems and water rights as well as mitigation efforts under water scarcity. Figure 12 shows K_c values sampled from hundreds of winter wheat fields in south central Idaho, where each vertical line represents a Landsat overpass date and each symbol represents a sampled field. The large black symbols represent a mean K_c averaged over all fields. High values early in the year represent fields that were more mature coming out of winter or were wet by irrigation. Sampled K_c during the middle of the year when most fields were at full cover had much lower variance about a mean. This type of sampling can be effective in producing actual K_c curves that best represent actual conditions for an area or for a year.

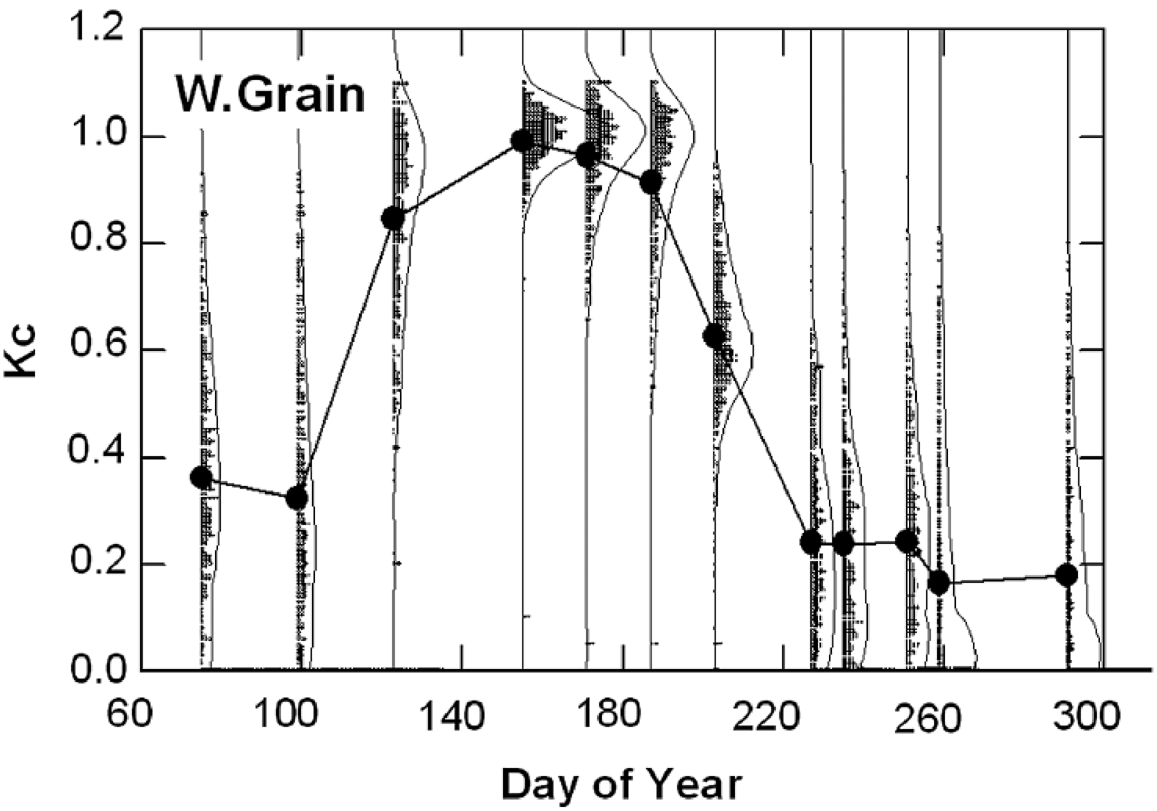

Figure 12. ***K_c* values sampled from hundreds of winter wheat fields in south central Idaho, where each vertical line represents a Landsat overpass date and each symbol represents a sampled field. The large black symbols represent a mean *K_c* averaged over all fields.**

Comparisons between remote sensing-based ET and traditional K_c ET_{ref}.

Figure 13 shows comparisons made between growing season ET_c calculated by METRIC and growing season ET using the K_c ET_{ref} method by the USBR AgriMet system for 2000, where AgriMet ET_c estimates were based on mean (single) K_c values traceable to Wright (1981). K_c ET_{ref} estimates were made for weather stations located near Twin Falls and Jerome, Idaho, which are 30 km apart.

The values shown for METRIC in Figure 13 were sampled from large numbers of fields in the Jerome and Twin falls counties from METRIC images of ET and K_c between the dates of March 15 and October 17 (Tasumi et al., 2005, Tasumi and Allen, 2007). The METRIC derived images were integrated monthly and over the March 1 – October 31 period. The 'Allen-Robison (2007)' entries in Figure 9 represent ET_c determined made using a dual crop coefficient x reference ET_r procedure and point weather data.

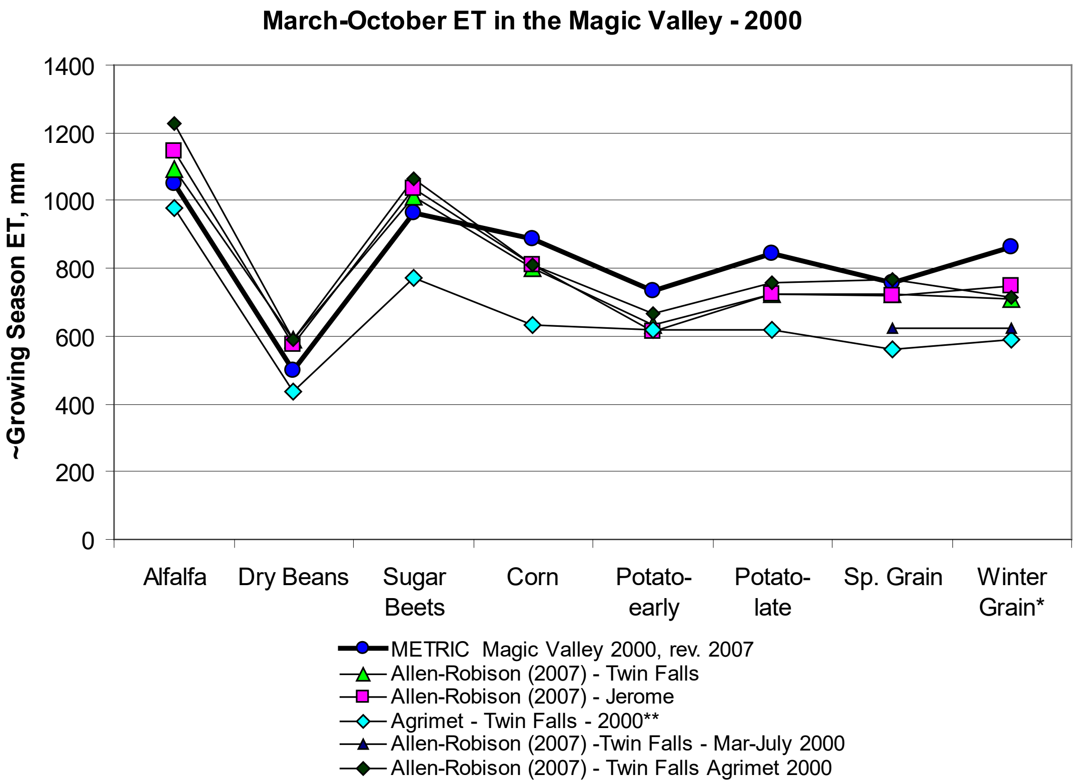

Figure 13. Growing season evapotranspiration during year 2000 for major crops grown in the Twin Falls – Jerome area of Magic Valley, Idaho from four sources (1. METRIC satellite-based energy balance; 2. Dual K_c x ET_{ref} (Allen-Robison 2007) for Twin Falls 7E and Jerome NWS stations; 3. USBR AgriMet ET reports based on K_{cm} x ET_{ref}.

Growing season ET_c from the dual K_c-based computations (averaged over Twin Falls and Jerome stations) were within 7% of METRIC estimates for alfalfa hay, sugar beets and spring grain and were within 16% of METRIC ET_c for all crops. The dual K_c-based estimates averaged about 16% above METRIC estimates for dry beans and 15-16% below METRIC estimates for winter grain and potatoes.

The lower ET_c estimation by Allen-Robison (2007) for corn and potatoes, relative to METRIC, stem partly from the assumption of relatively low-frequency irrigation scheduling when simulating irrigation schedules during estimation of soil evaporation. Corn crops tend to be irrigated by center pivot systems and potato crops by center pivots or by solid set sprinkler. Both of these system types tend to be operated so that irrigations are spaced more closely together in time than for wheel-line or gravity systems. The consequence of this is more frequent wetting of the soil surface and somewhat higher total ET_c. This may explain some of the 10 to 15% difference between the two estimating approaches. The 16% lower estimation for ET_c of winter wheat as compared to METRIC-produced ET_c appears to stem primarily from estimation of earlier crop development during early spring and earlier maturity and harvest estimated by the dual K_c process than observed by METRIC. An additional reason for the lower seasonal ET_c estimates by AgriMet is that their K_c and ET_c calculations do not begin until emergence (or greenup) and are discontinued at estimated harvest for annual crops. Therefore, evaporation from precipitation prior to and following the specific growing periods is neglected.

Future trends

Multilayer models

Future ET calculation may involve the use of multilayer ET models as cloud-based computing and intelligent simulation of vegetation over a growing season are developed, and include growth and fractions of ground cover. Multilayer ET models provide for separate parameterization of vegetation canopy and soil surfaces either as multiple sources of energy exchange or as inter-canopy blending formulations. The models generally employ aerodynamic and surface resistance formulations. Early derivations of multilayer models include Shuttleworth and Wallace (1985), Shuttleworth and Gurney (1990), and Dolman (1993). Those models have been widely tested and parameterized in research applications, but have not been widely used operationally due to the difficulty of establishing parameterizations for some of the internal resistances, which can change markedly with vegetation type and density and with time of year. Other challenges for the model include errors associated with impacts of unknown or unresolved surface temperature, T_s, on the slope of the saturation vapor pressure curve, Δ, outgoing long wave radiation, and within- and above-canopy aerodynamic stability correction. A highly recommended article on resistance model types is Daamen and McNaughton (2000), which describes and contrasts common formulations of model types and compares their estimated ET rates under several surface conditions.

Complexity in models can bring complexity in parameterization of the models. This can definitely be the case with multilayer and patch models where the characterization of heat and vapor transport within a canopy have, as a necessity, a degree of speculation and empiricism. If not formulated properly, these characterizations can induce more inaccuracy than accuracy (Were et al., 2008), especially if key factors such as buoyancy correction or penetration of air into the canopy by random eddy movement are not accounted for. For example, the required form and structure of formulations for internal resistances, r_h, may change with plant density, leaf area, vegetation patch size, wind speed, and buoyancy. For example, standard K theory (de Bruin et al., 1993) establishes nearly logarithmic wind speed and T and e profiles above some zero plane displacement height assuming expansive, open areas with well-established equilibrium boundary layers. However, the formulations may not be strictly applicable within canopies and along sudden patch boundaries. Also difficult to accurately account for is the horizontal transfer of sensible heat (and vapor deficit) from understory into canopy and vice versa.

Brenner and Incoll (1997) and Were et al., (2008) suggested a two-layer/three-source model with vegetation canopy, shaded soil, and exposed soil sources. One of the serious challenges in applying the multilayer or patch models to sparse vegetation systems is in the parameterization of r_h, which is the aerodynamic resistance within and across the canopy or near-surface boundary layers, and in the validity of applying the Penman-Monteith (PM) equation over this region. The traditional equations for aerodynamic resistances across T and e gradients assume that the T, e, and u profiles follow semilogarithmic shaped vertical profiles, the shapes of which are governed by surface roughness and density-induced buoyancies. However, within vegetation canopies, turbulent diffusion theory (K theory) (de Bruin et al., 1993) has been shown to be inadequate to describe convective transfer where even countergradient fluxes can exist (Raupach 1989; van den Hurk and McNaughton 1995; McNaughton and van den Hurk, 1995; Daamen and McNaughton, 2000). Therefore, empirical formulations have to be applied. The nature and structure of buoyancy correction within a sparse canopy is uncertain, even though it can constitute a very effective mechanism for transport of sensible heat and vapor upward within tall canopies such as trees, where mechanical mixing from wind is low due to sheltering. This increases uncertainty in applying multisource and multilayer models as formulated here.

Examples of patch models where the total surface is split into vegetation and exposed soil include the Energy-Water-Balance (ENWATBAL) model (Evett and Lascano, 1993; Lascano, 2000); a three-patch model by Brenner and Incoll (1997); and, using explicit equations for LE and H fluxes, the Two-Source-Energy-Balance (TSEB) model of Kustas (1990) and Kustas and Norman (1999) that is applied in a surface energy balance mode using thermal imagery, and a two-source patch model by Dhungel et al., (2016a; 2016b; 2019). The patch model was developed for simplicity (Delogu et al., 2018). However, because direct interchange between surface types is ignored, defining appropriate resistance values is often challenging. When vegetation patches are extensive in size, such that the microclimate of one patch does not affect the microclimate of another, then the aerodynamics and resistances of different surface types can be characterized by different roughness lengths and with quite different r_a values (Daamen and McNaughton, 2000).

Daamen and McNaughton (2000) show the patch and interactive models to have best agreement as canopy sparsity and patch size increase, for example with a lemon orchard, and agreement decreases with plant density and increasing ratios of aerodynamic resistance for momentum to aerodynamic resistance for sensible heat flux, r_{am} to r_h. They found higher evaporation estimated by the interactive model than by the patch model under some conditions due to interactions of fluxes between the component surfaces. As expected, the flux interactions are largest when the surface resistances for the soil and vegetation components are most different (for example, dry soil surface and well-watered canopy) and when r_{am} is larger than r_h and fractions of exposed soil and canopy are similar. When flux interactions are largest, differences between the single-layer and interactive (multilayer) models are the smallest.

In summary, this section describes some of the challenges with using the more complex multi-layer or multi-source ET models as compared to using the more empirical, but robust, crop coefficient models. However, in time, intelligent multi-layer modeling systems run on cloud-based computing systems may replace locally computed crop coefficient based calculation, with more accurate results. Implementation will require intelligence-based estimation of internal parameters via description of vegetation characteristics and environments. These types of models may also play a role, when coupled with gridded weather data, to interpolation of ET in between satellite image dates (Dhungel et al., 2016b).

Satellite-based remote sensing

Satellite-based remote sensing of ET will continue to evolve and find its way into common, operational water management. Satellite-based remote sensing has the advantage of 'seeing' actual ET under water short conditions and the ability to construct a historical database of actual ET. One impediment to satellite-based remote sensing that employs surface energy balance is the sparsity of high-resolution satellite systems such as Landsat that include a thermal sensor. More Landsat-class satellites are needed, with ideally a one-day revisit time, as compared to the current 8- or 16-day revisit time, to provide continuous assessment of thermal surface properties for creating near continuous snapshots of ET. This is especially important in the cloudier parts of the globe where a location may go weeks between clear days.

SUMMARY

The crop coefficient (K_c) and reference ET procedure for estimating ET has been very successful over the past 50 years due to its simplicity coupled with consistency and robustness. Much of this success has centered on the energy constraints represented in the reference ET. Modern applications are primarily centered on the FAO-56 dual K_c approach. Newer, and often preferred, bases for establishing K_{cb} curves include use of thermal units and vegetation-indices. Discussion is directed toward the application of reference ET calculation using hourly rather than 24-hour timesteps. The use of gridded weather data sets is becoming more widespread, but requires the conditioning of gridded weather data prior to calculation of reference ET. Future trends include the movement toward multi-layer and multi-source resistance models for ET estimation coupled with satellite-based determination of ET using both vegetation indices and surface energy balance.

REFERENCES

Abatzoglou, J.T. (2013). Development of gridded surface meteorological data for ecological applications and modelling. *International Journal of Climatology*, *33*(1), pp.121-131

Allen, R. G. (1996).“Nongrowing season evaporation in northern Utah. *Proc. N. Am. Water and Environ.Congr.*, Anaheim, CA, ASCE, New York, NY, pages].

Allen, R.G. (2011). Skin layer evaporation to account for small precipitation events—An enhancement to the FAO-56 evaporation model. *Agricultural Water Management*, *99*(1), pp.8-18.

Allen, R.G., & Pereira, L S. (2009). Estimating crop coefficients from fraction of ground cover and height. *Irrig. Sci.*, 28(1), 17–34.

Allen, R. G., & Robison, C.W. (2007). Evapotranspiration and consumptive irrigation water requirements for Idaho. *Univ. of Idaho Rep.*, submitted to the Idaho Dept. Water Resources, [location].

Allen, R.G., & Wright , J.L. (2006). Conversion of Wright (1981) and Wright (1982) alfalfa-based crop coefficients for use with the ASCE Standardized Penman-Monteith reference evapotranspiration equation. *Univ. of Idaho internal rept*. ‹http://www.kimberly.uidaho.edu/water/asceewri/Conversion_of_Wright_Kcs_2c.pdf›

Allen, R.G., Pereira, L S., Raes, D., & Smith M. (1998). Crop evapotranspiration: Guidelines for computing crop water requirements. *Irrig. and Drain. Paper No. 56*, United Nations Food and Agriculture Organization, Rome.

Allen, R.G., Tasumi, M., Morse, A. & Trezza, R. (2005). A Landsat-based energy balance and evapotranspiration model in Western US water rights regulation and planning. *Irrigation and Drainage systems*, *19*(3-4), pp.251-268.

Allen, R.G., Tasumi, M., & Trezza, R. (2007a). Satellite-based energy balance for mapping evapotranspiration with internalized calibration (METRIC)—Model. *Journal of irrigation and drainage engineering*, *133*(4), pp.380-394.

Allen, R.G., Tasumi, M., Morse, A., Trezza, R., Wright, J.L., Bastiaanssen, W., Kramber, W., Lorite, I., & Robison, C.W. (2007b). Satellite-based energy balance for mapping evapotranspiration with internalized calibration (METRIC)—Applications. *Journal of Irrigation and Drainage Engineering*, *133*(4), pp.395-406.

Allen, R.G., Pereira, LS., Howell, T. A., & Jensen, M.E. (2011a). Evapotranspiration Information Reporting: I. Factors Governing Measurement Accuracy. *Agricultural Water Management*. 98(6):899-920

Allen, R.G., Pereira, L.S., Howell, T.A., & Jensen, M.E. (2011b). Evapotranspiration Information Reporting: II. Recommended Documentation. *Agricultural Water Management.* 98(6):921-929.

Allen, R.G., Robison, C.W., Huntington, J.L., & Wright, J.L. (2020a). Applying the FAO56 dual Kc method for statewide irrigation water requirements and forecasting water demands. *Trans. ASABE* (in review).

Allen, R.G., Dhungel, R., Dhungira, B., & Huntington, J.L. (2020b). A boundary-layer-based procedure for conditioning gridded weather data to reflect weather measurements under irrigated conditions. *Agricultural Water Management*. (in review).

ASCE. (1990). *Evapotranspiration and irrigation water requirements*. Jensen, M.E., Burman, R.D., & Allen, R G. (ed.). ASCE Manuals and Reports on Engineering Practice No. 70, Reston, VA.

ASCE. (2005). *The ASCE standardized reference evapotranspiration equation.* Task Committee on Standardized Calculation of Reference Evapotranspiration Calculation, EWRI, Reston, VA.

ASCE. (2016). *Evaporation, evapotranspiration, and irrigation water requirements*. American Society of Civil Engineers. Jensen, M.E. and Allen, R.G. eds., 2016, 770 p.

Bastiaanssen, W. G. M., Noordman, E. J. M., Pelgrum, H., Davids, G., Thoreson, B. P., & Allen, R. G. (2005). SEBAL model with remotely sensed data to improve water resources management under actual field conditions. *J. Irrig. and Drain. Eng.*, 131(1), 85–93.

Betts, A.K., Chen, F., Mitchell, K.E., & Janjić, Z.I. (1997). Assessment of the land surface and boundary layer models in two operational versions of the NCEP Eta model using FIFE data. *Monthly Weather Review*, *125*(11), pp.2896-2916.

Blankenau, P. A., Kilic, A., & Allen, R. (2020). An evaluation of gridded weather data sets for the purpose of estimating reference evapotranspiration in the United States. *Agricultural Water Management*, 242, 106376.

Brown, P.W., et al. (2001). Penman Monteith crop coefficients for use with desert turf systems. *Crop Sci*., 41, 1197–1206.

Burt, C.M., Mutziger, A J., Howes, D.J., & Solomon, K H. (2005a). “Evaporation from irrigated agricultural land in California.” [publisher, location]

Cesaraccio, C., Spano, D., Duce, P., & Snyder, R L. (2001). An improved model for degree-days from temperature data. *Int'l. J.*

Biometeorol., 45(4), 161–169.

Daamen, C. C., & McNaughton, K. G. (2000). Modeling energy fluxes from sparse canopies and understorys. *Agron. J.,* 92, 837–847.

De Bruin, H. A. R., Kohsiek, W., & Van Den Hurk, B. J. J. M. (1993). A verification of some methods to determine the fluxes of momentum, sensible heat, and water vapour using standard deviation and structure parameter of scalar meteorological quantities. *Boundary-Layer Meteorology*, 63(3), 231-257.

Delogu, E., Boulet, G., Olioso, A., Garrigues, S., Brut, A., Tallec, T., ... & Lagouarde, J. P. (2018). Evaluation of the SPARSE dual-source model for predicting water stress and evapotranspiration from thermal infrared data over multiple crops and climates. *Remote Sensing*, 10(11), 1806.

Dhungel, R., Allen, R. G., & Trezza, R. (2016a). Improving iterative surface energy balance convergence for remote sensing based flux calculation. Journal of Applied Remote Sensing, 10(2), 026033.

Dhungel, R., Allen, R.G., Trezza, R., & Robison, C.W. (2016b). Evapotranspiration between satellite overpasses: methodology and case study in agricultural dominant semi-arid areas. *Meteorological Applications*, *23*(4), pp.714-730.

Dhungel, R., Aiken, R., Colaizzi, P. D., Lin, X., O'Brien, D., Baumhardt, R. L., ... & Marek, G. W. (2019). Evaluation of uncalibrated energy balance model (BAITSSS) for estimating evapotranspiration in a semiarid, advective climate. Hydrological Processes, 33(15), 2110-2130.

Doorenbos, J., & Pruitt, W. O. (1977). Guidelines for predicting crop water requirements. *FAO Irrig. and Drain.* Paper No. 24, 2nd Ed., Food and Agriculture Organization, United Nations, Rome.

Erie, L J., French, O.F., & Harris, K. (1965). Consumptive use of water by crops in Arizona. *Univ. of Ariz. Agri. Exp. Sta. Tech. Bull. 169*,

Erie, L .J., French, O. F., Bucks, D. A., and Harris, K. (1982). Consumptive use of water by major crops in the southwestern United States. *Conservation Res. Rep. No. 29,* USDA, [location].

Flerchinger, G N. (1991). Sensitivity of soil freezing simulated by the SHAW Model. *Trans. of the ASAE*, 34(6), 2381–2389.

Flerchinger, G.N., Hanson, C.L., & Wight, J.R. (1996). Modelling of evapotranspiration and surface energy budgets across a watershed. *Water Resour. Res*., 32(8), 2539–2548.

Flesch, T.K., & Dale, R.F. (1987). A leaf area index model for corn with moisture stress reductions. *Agron. J.*, 19, 1008–1014.

French, A.N., Hunsaker, D.J., and Thorp, K.R. 2(015). Remote sensing of evapotranspiration over cotton using the TSEB and METRIC energy balance models. *Remote Sensing of Environment*, *158*, pp.281-294.

Hargreaves, G. H. (1948). Irrigation requirement data for Central Valley crops. U.S. Bur. of Recl., Branch of Proj. Planning, Sacramento, CA.

Hidalgo, H.G., Cayan, D.R., & Dettinger, M.D. (2005). Sources of Variability of Evapotranspiration in California. J. Hydrometeor, 6, 3–19

Hunsaker, D.J. (1999). Basal crop coefficients and water use for early maturity cotton. *Trans. of the ASAE,* 42(4), 927–936.

Huntington, J. L., Gangopadhyay, S., Spears, M., Allen, R. G., King, D., Morton, C., Harrison, A., McEvoy, D., & Joros, A. (2015). West-Wide Climate Risk Assessments: Irrigation Demand and Reservoir Evaporation Projections. Bureau of Reclamation, Technical memorandum No. 68-68210-2014-01, 196p., 841 app, http://www.usbr.gov/watersmart/wcra/

Huntington, J. L., Morton, C. G., McEvoy, D., Bromley, M., Hedgewisch, K., Allen, R.G., & Gangopadhyay, S. (2016). Historical and Future Irrigation Water Requirements for Select Reclamation Project Areas of the Western United States. U.S. Department of the Interior Bureau of Reclamation. USA. 87 p. https://www.usbr.gov/watersmart/baseline/docs/irrigationdemand/irrigationdemands.pdf. Appendices are at https://www.usbr.gov/watersmart/baseline/docs/irrigationdemand/Appendices.pdf.

Jacobs, C.M.J., & de Bruin, H.A.R. (1997). Predicting regional transpiration at elevated atmospheric CO2: Influence of the PBL vegetation interaction. *J. Appl. Meteorol. Clim.*, 36, 1663–1675.

Jensen, D.T., Hargreaves, G.H., Temesgen, B., & Allen, R.G. (1997). Computation of ETo under nonideal conditions. *Journal of Irrigation and Drainage Engineering*, *123*(5), pp.394-400.

Jensen, M.E. (1968). Water consumption by agricultural plants. *Water deficits and plant growth*, Kozlowski, T. T., ed., Vol. II, Academic Press, New York, 1–22.

Jensen, M. E. (1969). Scheduling irrigations with computers. *J. Soil and Water Conserv.*, 24(5), 193–195.

Jensen, M.E., & Allen, R.G. eds. (2016), April. Evaporation, evapotranspiration, and irrigation water requirements. American Society of Civil Engineers. 775 p.

Jensen, M.E., Robb, D.C.N., & Franzoy, C.E. (1970). Scheduling irrigations using climate-crop-soil data. *J. Irrig. and Drain. Div.*, 96, 25–28.

Jensen, M E., & Erie, L J. (1971). Irrigation and water management. *Advances in Sugarbeet Production*, Johnson, R. T. et al., eds. Iowa State Univ. Press, Ames, IA, 189–222.

Jensen, M.E., Burman, R.D., & Allen, R G. (1990). Evapotranspiration and irrigation water requirements. *ASCE Manuals and Reports on Engineering Practice No. 70,* Reston, VA.

Johnson, L.F., Cahn, M., Martin, F., Melton, F., Benzen, S., Farrara, B., & Post, K. (2016). Evapotranspiration-based irrigation scheduling of head lettuce and broccoli. *HortScience*, *51*(7), pp.935-940.

Kalma, J.D., McVicar, T.R., & McCabe, M.F. (2008). Estimating land surface evaporation: A review of methods using remotely sensed surface temperature data. *Surveys in Geophysics*, *29*(4-5), pp.421-469.

Karimi, P. & Bastiaanssen, W.G. (2015). Spatial evapotranspiration, rainfall and land use data in water accounting--Part 1: Review of the accuracy of the remote sensing data. *Hydrology & Earth System Sciences*, *19*(1).

Kilic-Irmak, A., Ratcliffe, I., Ranade, P., Irmak, J.S., Allen, R.G., Kjaersgaard, J., ... & Mutiibwa, D. (2012). Seasonal evapotranspiration mapping using Landsat visible and thermal data with an energy balance approach in central Nebraska. *Remote Sensing and Hydrology*, 352, 84-88.

Kilic, A., & Allen, R.G. (2015). Google Earth Engine Evapotranspiration Flux --- EEFlux. Slide no. 13 of http://arquivos.ana.gov.br/imprensa/eventosprojetos/20150904_Kilic_Allen_EEFlux_ANA_Brasilia_2015a.pdf\ also as Slide no. 7. https://landsat.usgs.gov/sites/default/files/documents/Allen_UNL_DRI_UI_EEFlux_update_LST_meeting_July_8_2015c.pdf

Kjaersgaard, J., Allen, R., & Irmak, A. (2011). Improved methods for estimating monthly and growing season ET using METRIC applied to moderate resolution satellite imagery. *Hydrological Processes*, 25(26), 4028-4036.

Lascano, R. J. (2000). A general system to measure and calculate daily water use. *Agron. J.*, 92(5), 821–832.

Martin, D. L., & Gilley, J. (1993). Irrigation water requirements. Chap. 2, Part 623, *National engineering Handbook*, Soil Conservation Service, USDA.

Melton, F.S., Johnson, L.F., Lund, C.P., Pierce, L.L., Michaelis, A.R., Hiatt, S.H., Guzman, A., Adhikari, D.D., Purdy, A.J., Rosevelt, C., & Votava, P. (2012). Satellite irrigation management support with the terrestrial observation and prediction system: A framework for integration of satellite and surface observations to support improvements in agricultural water resource management. *IEEE Journal of Selected Topics in Applied Earth Observations and Remote Sensing*, *5*(6), pp.1709-1721

Mitchell, K. E., et al. (2004). The multi-institution North American Land Data Assimilation System (NLDAS): Utilizing multiple GCIP products and partners in a continental distributed hydrological modeling system. *J. Geophys. Res.,* 109, D07S90, doi:10.1029/2003JD003823.

Overgaard, J., Rosbjerg, D., & Butts, M.B. (2006). Land-surface modelling in hydrological perspective? a review. hal.archives-ouvertes.fr

Pereira, L.S., Paredes, P., Melton, F., Johnson, L., Wang, T., Lopez-Urrea, R., Cancela, J.J., & Allen, R.G. (2020). Predication of crop coefficients from fraction of ground cover and height. Background and validation using ground and remote sensing data. *Ag. Water Man.* hpps://doi.org/10.1016/].agwat.2020.106197 .

Ranade, P. (2010). Spatial Water Balance for Bare Soil. University of Nebraska. Report, 10

Ritchie, J.T. (1974)."Evaluating irrigation needs for southeastern U.S.A. *Proc., Irrig. and Drain. Spec. Conf.*, ASCE, [location], 262–273.

Ritchie, J.T. (1991). Wheat phasic development. In Hanks, R.J., and Ritchie, J.T., eds., "Modeling plant and soil systems." *Agron. Series No. 31,* Am. Soc. Agron., Madison, WI, 31–54.

Ritchie, J. ., & NeSmith, D.S. (1991). Temperature and crop development. *Agronomy Series No. 31,* Hanks, R. J., and Ritchie, J. T., eds., Am. Soc. Agron., Madison, WI, 5–29.

Said, W., Jacobs, J., Irizarry-Ortiz, M.M, Trimble, P., Obeysekera., J., Tarboton, K., & Moustafa, Z. (2006). Appendix D, Estimation of long-term reference evapotranspiration for hydrologic modeling. Sept. 28, 2006 draft, hydrologic and Environmental Systems Modeling. South Florida Water Management District. 78 p.

Sammis, T.W. (1985). "Evapotranspiration crop coefficients predicted using growing-degree-days." *Trans. of the ASAE*, 28(3), 773–780.

Sammis, T.W., Mexal, J.G., & Miller, D. (2004). Evapotranspiration of flood-irrigated pecans. *Agric. Water Manage.*, 69, 179–190.

Saxton, K.E., & Willey, P.H. (2005). The SPAW model for agricultural field and pond hydrologic simulation. *Mathematical modeling of watershed hydrology*, Singh, V.P., and Frevert, D., eds., CRC Press,

Senay, G.B., Verdin, J.P., Lietzow, R., & Melesse, A.M. (2008). Global daily reference evapotranspiration modeling and validation. *J. Am. Water Resources Res.,* 44(4), 969–979.

Sinclair, T.R. (1984). Leaf area development in field-grown soybeans. *Agron. J.*, 76, 141–146.

Singh, R. K., & Kilic-Irmak, A. (2009). Estimation of crop coefficients using satellite remote sensing. *Journal of Irrigation and Drainage Engineering*, ASCE. 135(5), 597-608.

Slack, D C., Martin, E.C., Sheta, A.E., Fox F., Jr., Clark, L J., & Ashley, R.O. (1996). Crop coefficients normalized for climatic variability with growing-degree-days." *Proc. Int'l. Conf. on Evapotranspiration and Irrigation Scheduling,* San Antonio, TX, ASAE, St. Joseph, MI, 892–898.

Snyder, R L. (1985). Hand calculating degree days. *Agr. and For. Meteorol.*, 35, 353–358

Snyder, R.L, & Eching, S. O. (2005) Urban landscape evapotranspiration. *Calif. Water Plan Update 2005,* 4, 691–693.

Snyder, R.L., Spano, D., Cesaraccio, C., & Duce, P. (1999). Determining degree-day thresholds from field observations. *Int. J. Biomet*., 42, 177–182.

Spano, D., Cesaraccio, C., Duce, P., & Snyder, R.L. (2002). An improved model for estimating degree days. *ISHS Acta Horticulturae 584: VI International Symposium on Computer Modelling in Fruit Research and Orchard Management*, [location, pages/paper #].

Tasumi, M., & Allen, R.G. (2007). Satellite-based ET mapping to assess variation in ET with timing of crop development. *Agricultural Water Management*, *88*(1-3), pp.54-62.

Tasumi, M., Allen, R.G., Trezza, R., & Wright, J.L. (2005). Satellite-based energy balance to assess within-population variance of crop coefficient curves. *Journal of irrigation and drainage engineering*, *131*(1), pp.94-109.

Temesgen, B., Allen, R.G., & Jensen, D.T. (1999). Adjusting temperature parameters to reflect well-watered conditions. *Journal of Irrigation and Drainage Engineering*, *125*(1), pp.26-33.

Tolk, J.A., Howell, T.A., & Evett, S.R. (2006). Nighttime evapotranspiration from alfalfa and cotton in a semiarid climate. *Agron J.*, 98, 730–736.

U.S. Department of Agriculture (USDA). (1967). Irrigation water requirements. *Soil Conserv. Service. Tech. Rel. No. 21,* Washington, DC.

Veihmeyer, F.J., & Hendrickson, A H. (1955). Does transpiration decrease as the soil moisture decreases? *Trans. Amer. Geophy. Un*., 36, 425–448.

Were, A., Villagarcia, L., Domingo, F., & Moro, M.J. (2008). Aggregating spatial heterogenity in a bush vegetation patch in semi-arid SE Spain: A multi-layer model versus a single-layer model. *J. of Hydrology*, 349(1–2):156–167.

Wigmosta, M.S., Vail, L.W., & Lettenmaier, D.P. (1994). A distributed hydrology-vegetation model for complex terrain. *Water resources research*, *30*(6), pp.1665-1679.

Wright, J.L. (1981). Crop coefficients for estimates of daily crop evapotranspiration. *Irrig. Sched. for Water and Energy Conserv. in the 80s*, ASAE,, Dec. 18–26.

Wright, J.L. (1982). New evapotranspiration crop coefficients. *J. Irrig. and Drain. Div.*, 108(2), 57–74.

Wright, J.L. (1993). Nongrowing season ET from irrigated fields. *Management of Irrigation and Drainage Systems*, Proc. ASCE Spec. Conf. Park City, UT, July 21–23, [location of publisher/sponsor],1005–1014.

Wright, J.L. (2001). Growing degree day functions for use with evapotranspiration crop coefficients. Agronomy abstracts (CD-ROM). American Society of Agronomy, [location].